

AD-A188 821

INVESTIGATION OF DEFECT AND ELECTRONIC INTERACTIONS  
ASSOCIATED WITH GART (U) MASSACHUSETTS INST OF TECH  
CAMBRIDGE DEPT OF MATERIALS SCIENCE H C GATOR ET AL.  
AUG 87 AFOSR-IR-87-1986 AFOSR-86-8342 P/G 7/2

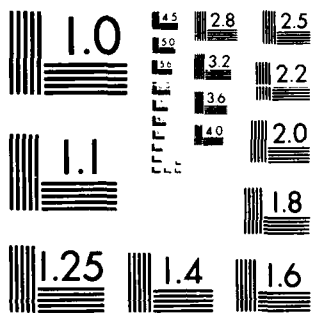
1/1

UNCLASSIFIED

ML

END  
DATE  
FILMED  
28

182



MICROCOPY RESOLUTION TEST CHART  
NATIONAL BUREAU OF STANDARDS 1963-A

UNCLASSIFIED

2

AD-A188 021

REPORT DOCUMENTATION PAGE

DTIC FILE COPY

2a. SECURITY CLASSIFICATION AUTHORITY		DTIC ELECTED		1b. RESTRICTIVE MARKINGS	
2b. DECLASSIFICATION/DOWNGRADING SCHEDULE		JAN 14 1988		3. DISTRIBUTION/AVAILABILITY OF REPORT Approved for public release; distribution unlimited.	
4. PERFORMING ORGANIZATION REPORT NUMBER(S)		H		5. MONITORING ORGANIZATION REPORT NUMBER(S) AFOSR-TR. 87-1906	
6a. NAME OF PERFORMING ORGANIZATION Dr. Jacek Lagowski/ Prof. Harry C. Gatos		6b. OFFICE SYMBOL (If applicable)		7a. NAME OF MONITORING ORGANIZATION Same as 8A	
6c. ADDRESS (City, State and ZIP Code) Massachusetts Institute of Technology 77 Massachusetts Ave. Cambridge, MA 02139				7b. ADDRESS (City, State and ZIP Code) Same as 8c	
8a. NAME OF FUNDING/SPONSORING ORGANIZATION AFOSR		8b. OFFICE SYMBOL (If applicable) NE		9. PROCUREMENT INSTRUMENT IDENTIFICATION NUMBER AFOSR-86-0342	
8c. ADDRESS (City, State and ZIP Code) Bldg 410 Bolling Air Force Base, D.C. 20332		10. SOURCE OF FUNDING NOS.			
		PROGRAM ELEMENT NO. 61102F	PROJECT NO. 2306	TASK NO. B1	WORK UNIT NO.
11. TITLE (Include Security Classification) Investigation of Defect & Elec. Interactions Associated with GaAs Device Processing					
12. PERSONAL AUTHOR(S) Prof. Harry C. Gatos and Dr. Jacek Lagowski					
13a. TYPE OF REPORT Annual		13b. TIME COVERED FROM 8/16/86 TO 8/15/87		14. DATE OF REPORT (Yr., Mo., Day) 1987/November/10 AUG	
15. PAGE COUNT 7					
16. SUPPLEMENTARY NOTATION					
17. COSATI CODES			18. SUBJECT TERMS (Continue on reverse if necessary and identify by block number)		
FIELD	GROUP	SUB. GR.			
19. ABSTRACT (Continue on reverse if necessary and identify by block number) In our research on new semi-insulating behavior in III-V compounds we have essentially completed the determination of electronic levels and related optical properties of substitutional titanium in bulk-grown InP and GaAs. In the course of the corresponding crystal growth study we have also identified impurity gettering by transition elements. This gettering takes place due to chemical reactions between transition elements and impurities in the growth melt (or solution), and it can be beneficial or detrimental for obtaining SI materials. An example of the beneficial role is provided by the interaction of vanadium with silicon, which reduces Si donor concentration in the grown crystal. An example of detrimental effect is provided by the interaction of titanium with carbon, which reduces the concentration of deep compensating Ti donors in epitaxial or melt-grown crystals. This problem must be overcome in order to achieve controllable Ti doping of the crystals. Appropriate redesign of the epitaxial growth cell (eliminating all graphite elements in contact with the solution) is in progress. In parallel, we have carried out an investigation on the extension					
20. DISTRIBUTION/AVAILABILITY OF ABSTRACT UNCLASSIFIED/UNLIMITED <input checked="" type="checkbox"/> SAME AS RPT. <input type="checkbox"/> DTIC USERS <input type="checkbox"/>			21. ABSTRACT SECURITY CLASSIFICATION UNCLASSIFIED		
22a. NAME OF RESPONSIBLE INDIVIDUAL CAPT MALLOY		22b. TELEPHONE NUMBER (Include Area Code) 202/767-4931		22c. OFFICE SYMBOL NE	

of liquid phase electroepitaxy to the growth of bulk InGaAs crystals. We have successfully developed procedures for the electroepitaxial growth of  $\text{In}_{0.52}\text{Ga}_{0.48}\text{As}$  ingots 14 mm in diameter and up to 3 mm thick. To our knowledge, these are the first bulk InGaAs crystals to show excellent compositional uniformity (in accord with theoretical predictions for electroepitaxy).

APPROX. 10.52 - 0.48

AFOSR-TR- 87-1906

ANNUAL TECHNICAL REPORT

to

AIR FORCE OFFICE OF SCIENTIFIC RESEARCH  
BOLLING AIR FORCE BASE, D. C. 20332

on

INVESTIGATION OF DEFECT AND ELECTRONIC INTERACTIONS  
ASSOCIATED WITH GaAs DEVICE PROCESSING

(AFOSR-86-0342)

For Period

August 16, 1986 to August 15, 1987

Submitted by

Professor Harry C. Gatos  
and  
Dr. Jacek Lagowski  
Department of Materials Science and Engineering  
Massachusetts Institute of Technology  
Cambridge, Massachusetts 02139



Accession For	
NTIS GRA&I	<input checked="" type="checkbox"/>
DTIC TAB	<input type="checkbox"/>
Unannounced	<input type="checkbox"/>
Justification	
By	
Distribution/	
Availability Codes	
Dist	Avail and/or Special
A-1	

87 12 29 232

## I. SUMMARY

In our research on new semi-insulating behavior in III-V compounds we have essentially completed the determination of electronic levels and related optical properties of substitutional titanium in bulk-grown indium phosphide and gallium arsenide. In the course of the corresponding crystal growth study we have also identified impurity gettering by transition elements. This gettering takes place due to chemical reactions between transition elements and impurities in the growth melt (or solution), and it can be beneficial or detrimental for obtaining SI materials. An example of the beneficial role is provided by the interaction of vanadium with silicon, which reduces Si donor concentration in the grown crystal. An example of detrimental effect is provided by the interaction of titanium with carbon, which reduces the concentration of deep compensating Ti donors in epitaxial or melt-grown crystals. This problem must be overcome in order to achieve controllable Ti doping of the crystals. Appropriate redesign of the epitaxial growth cell (eliminating all graphite elements in contact with the solution) is in progress. In parallel, we have carried out an investigation on the extension of liquid phase electroepitaxy to the growth of bulk InGaAs crystals. We have successfully developed procedures for the electroepitaxial growth of  $\text{In}_{0.52}\text{Ga}_{.48}\text{As}$  ingots 14 mm in diameter and up to 3 mm thick. To our knowledge, these are the first bulk InGaAs crystals to show excellent compositional uniformity (in accord with theoretical predictions for electroepitaxy).

We have also developed a new optical approach for the characterization of semi-insulating GaAs in terms of Fermi energy and other key parameters.

The results of our activity are outlined below and are discussed in the publications enclosed with this report.

### 1. Electronic Levels and Optical Properties of Ti

We have essentially completed the identification of the electronic levels and corresponding optical transitions of Ti in GaAs and InP. The data on electronic levels are summarized in Fig. 1. Corresponding optical transitions observed in GaAs are shown in Fig. 2. They involve: electron photoionization transitions  ${}^3A_2 \rightarrow \text{C.B.}$  and  ${}^2E \rightarrow \text{C.B.}$  from  $\text{Ti}^{2+}$  acceptor and  $\text{Ti}^{3+}$  donor, respectively; corresponding hole photoionization transitions  $\text{V.B.} \rightarrow {}^2E$  and  $\text{V.B.} \rightarrow {}^3A_2$ ; and intracenter transitions. In InP the  $\text{Ti}^{2+}$  acceptor is located in the conduction band, thus only the transitions corresponding to the  $\text{Ti}^{3+}$  donor are observed.

Extensive crystal growth experiments have led to the determination of the effective segregation coefficient for the growth from the melt of about  $(3 \pm 1) \times 10^{-5}$  for GaAs and  $(5 \pm 2) \times 10^{-4}$  for InP.

The midgap energy position of the  $\text{Ti}^{3+}$  donor combined with the segregation coefficient larger than that for GaAs made it possible to develop a formulation for producing a new type of semi-insulating InP based on doping with Ti and co-doping with acceptors. Resistivities in excess of  $10^7 \Omega\text{cm}$  were obtained with this procedure. SI-Ti:InP showed good thermal stability during thermal annealing consistent with expected low diffusivity of Ti.

Detailed discussion of the results is given in the Ph.D. thesis of C.D. Brandt (ref. 1) and a forthcoming publication (ref. 2).

### 2. Gettering Action of Transition Metals

We have discovered the gettering of shallow donor impurities by vanadium. It was found that vanadium doped in the growth melt gettered silicon and sulfur through chemical interaction and led to the reduction in the concentration of free electrons and enhancement of the mobility value (see Fig. 3). Thus, by controlled doping of the growth melt with vanadium semi-insulating GaAs

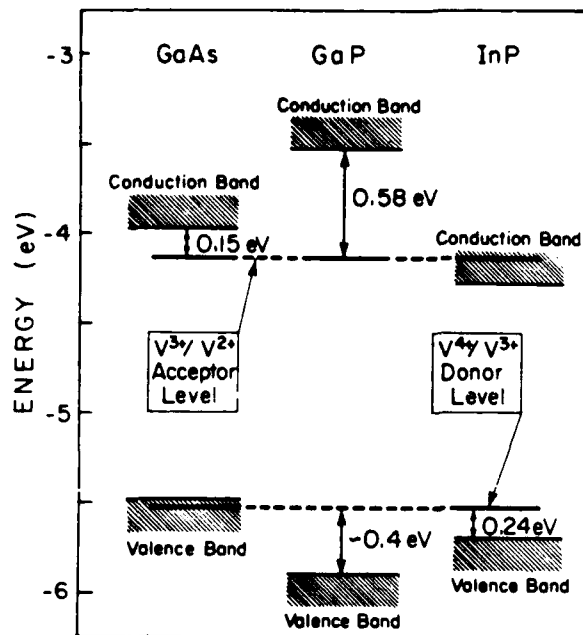
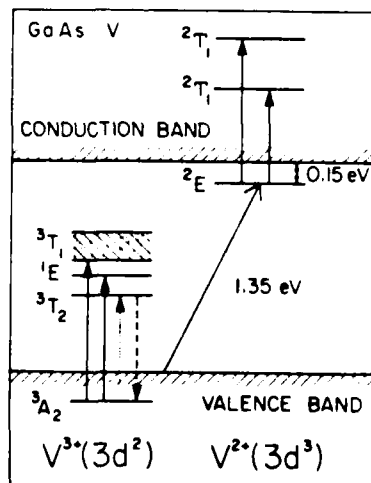


Figure 1.

Vacuum-related binding energies of the vanadium-donor and -acceptor levels in some III-V compounds. The vanadium-donor level in GaP has not yet been observed, but is predicted to lie at  $E_v + 0.4$  eV.



Energy levels of the  $V^{3+}(3d^2)$  and  $V^{2+}(3d^3)$  charge states in GaAs. Vertical arrows represent intracenter transitions and the slanted arrow represents the charge transfer:  $V^{3+}(3d^2) + e^- \Rightarrow V^{2+}(3d^3)$ . The indicated level symmetries have been taken from Ref 25.

Figure 2.

crystals were reproducibly grown by both the Horizontal Bridgman and Liquid Encapsulated Czochralski techniques. Our previous study (ref. 3) demonstrated that vanadium does not introduce any midgap levels which could contribute to the electrical compensation. The high resistivity reported in the literature for certain V-doped GaAs crystals must originate from the presently discovered gettering effect.

No evidence was found for Si or S gettering by Ti. However, titanium interaction with carbon present in the growth system (graphite elements of LPEE apparatus and/or carbon in the GaAs melt) has a negative effect. It decreases Ti concentration in the grown crystal and also decreases the concentration of carbon acceptors. In view of these findings we are modifying the LPEE growth apparatus replacing or minimizing the graphite elements.

### 3. LPEE Growth of Bulk Ternary III-V Compounds

In order to achieve electroepitaxial growth of thick crystals of ternary III-V compounds (suitable for subsequent slicing to wafers) we had to overcome the problems associated with the preparation of the source material of desired composition and homogeneity. In this study the homogenous source pellets were prepared by rapid cooling of the quasibinary mixture, InAs-GaAs. Using a modified growth cell  $\text{In}_{1-x}\text{Ga}_x\text{As}$  ingots were subsequently grown 14 mm in diameter and up to 3 mm thick (ref. 4). As shown in Fig. 4, the ingot shows excellent compositional uniformity which to the best of our knowledge is unobtainable by any other growth method.

This successful adaptation of LPEE to growth of bulk ternary compounds must be considered an important technological spin-off of our program.

### 4. Characterization

We have developed a characterization approach based on the optical measurements of 1.039 eV zero phonon line intensity, which makes it possible to

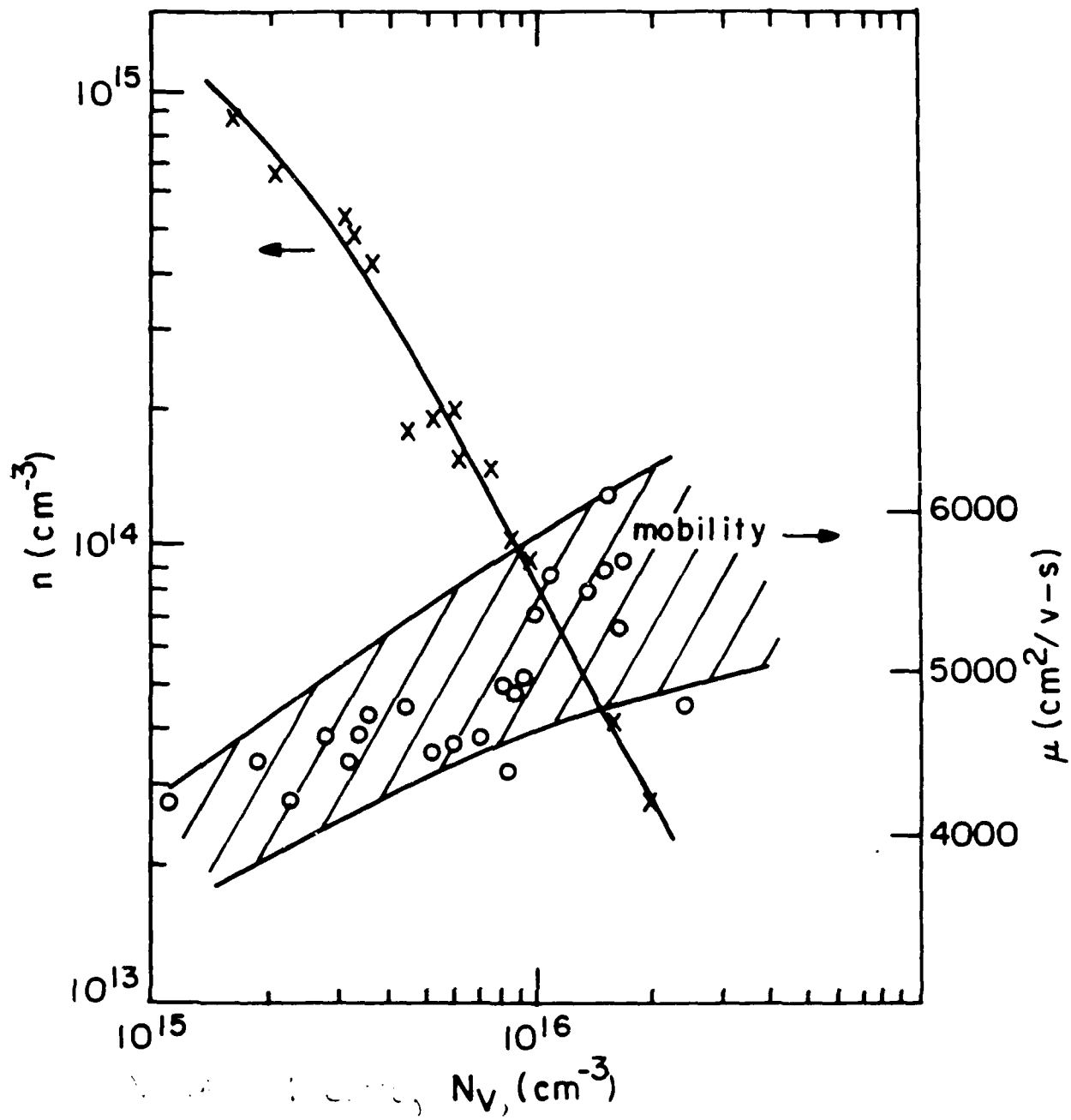


Figure 3.

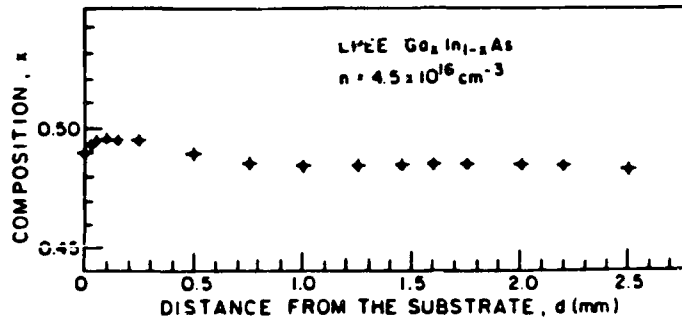
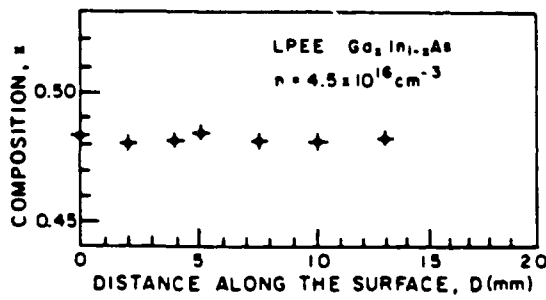


Fig. 4. Composition profile of  $\text{In}_{0.52}\text{Ga}_{0.48}\text{As}$  obtained from PL measurements:  
 (a) along the growth direction



(b) perpendicular to the growth direction.

determine the key electronic characteristics of semi-insulating GaAs, i.e., the Fermi energy, concentration and occupancy of EL2, and the net concentration of ionized acceptors (ref. 6).

#### REFERENCES

1. "A Study of Energy Levels Introduced by 3d Transition Elements in III-V Compound Semiconductors," C.D. Brandt, Ph.D. Thesis, MIT, June 1987.
2. C.D. Brandt, A.M. Hennel, J. Lagowski, and H.C. Gatos, "Optical and Electronic Properties of Vanadium in GaAs and InP," in preparation for publication.
3. A.M. Hennel, C.D. Brandt, K.Y. Ko, J. Lagowski, and H.C. Gatos, "Optical and Electronic Properties of Vanadium in Gallium Arsenide," J. Appl. Phys. 62, 163 (1987).
4. T. Bryskiewicz, M. Bugajski, B. Bryskiewicz, J. Lagowski, and H.C. Gatos, "LPEE Growth and Characterization of  $\text{In}_{1-x}\text{Ga}_x\text{As}$  Bulk Crystals," Proc. GaAs and Related Compounds, Crete, Greece, Sept. 1987.
5. C.H. Kang, K. Kondo, J. Lagowski, and H.C. Gatos, "Arsenic Ambient Conditions Preventing Surface Degradation of GaAs during Capless Annealing at High Temperatures," J. Electrochem. Soc. 134, 1261 (1987).
6. J. Lagowski, M. Bugajski, M. Matsui, and H.C. Gatos, "Optical Characterization of Semi-insulating GaAs; Determination of the Fermi Energy, the Concentration of the Midgap EL2 Level, and Its Occupancy," Appl. Phys. Lett. 51, 511 (1987).

## Optical and electronic properties of vanadium in gallium arsenide

A. M. Hennel,<sup>a)</sup> C. D. Brandt, K. Y. Ko, J. Lagowski, and H. C. Gatos  
*Massachusetts Institute of Technology, Cambridge, Massachusetts 02139*

(Received 15 January 1987; accepted for publication 10 March 1987)

The effects of vanadium doping on the electrical and optical properties of GaAs were systematically studied in melt-grown crystals prepared by the liquid-encapsulated Czochralski and horizontal Bridgman techniques and in epitaxial crystals prepared by liquid-phase electroepitaxy. By employing deep-level transient spectroscopy, Hall-effect measurements and the  $V^{2+}(3d^3)$  and  $V^{3+}(3d^2)$  intracenter optical-absorption spectra, one vanadium-related level was identified in all crystals, i.e., the substitutional-vanadium acceptor level ( $V^{3+}/V^{2+}$ ) at  $0.15 \pm 0.01$  eV below the bottom of the conduction band. From the absorption measurements we conclude that the vanadium ( $V^{4+}/V^{3+}$ ) donor level must be located within the valence band. Because of its energy position, the above level cannot account for the reported semi-insulating properties of V-doped GaAs. We observed no midgap levels resulting from vanadium-impurity (defect) complexes. The high resistivity reported for certain V-doped GaAs crystals must result from indirect effects of vanadium, such as the gettering of shallow-level impurities.

### I. INTRODUCTION

In the last few years several laboratories have reported the successful growth of semi-insulating (SI) V-doped GaAs, emphasizing its potential for improving device-processing characteristics relative to Cr-doped GaAs.<sup>1</sup> SI V-doped GaAs crystals have been grown by liquid-encapsulated Czochralski (LEC),<sup>2-5</sup> vapor-phase epitaxy (VPE),<sup>6</sup> and metallo-organic chemical vapor deposition (MOCVD)<sup>7,8</sup> techniques. The growth of low-resistivity V-doped GaAs crystals by LEC<sup>9,10</sup> and horizontal Bridgman (HB)<sup>5,11</sup> techniques has also been reported. In the above studies the positions of the energy levels tentatively attributed to vanadium range from near the conduction band edge<sup>9-12</sup> to midgap.<sup>2,6,7</sup>

It has also been shown<sup>13,14</sup> that the diffusivity of vanadium in GaAs is about one order of magnitude lower than that of chromium. On the basis of this finding and the report of a level at  $E_c + 0.58$  eV in V-doped VPE GaAs,<sup>6</sup> a compensation mechanism for V-doped SI GaAs was proposed.<sup>13,14</sup> These reports also concluded that V-doped SI GaAs would be superior in quality to all other commercially available types of SI GaAs crystals.

In this paper we discuss the effects of vanadium on the properties of GaAs based on the results of studies carried out on a series of V-doped melt- and solution-grown GaAs crystals using different growth and doping conditions. We show that the only vanadium-related level within the GaAs energy gap is an acceptor level at 0.15 eV below the conduction band. Some preliminary results have already been presented.<sup>15-17</sup>

### II. EXPERIMENTAL PROCEDURES

Vanadium-doped melt-grown GaAs crystals were prepared by the LEC and HB techniques by using both pyrolytic boron nitride (PBN) and quartz crucibles. Two different

types of crucibles were used in order to test the hypothesis that inconsistencies in the reported data resulted from interactions of vanadium with impurities originating in the crucible. (For example, SI LEC GaAs crystals were grown by Wacker-Chemicronic with the use of quartz crucibles.<sup>4,13</sup>) Doping with vanadium at concentrations reaching a level of  $3 \times 10^{19} \text{ cm}^{-3}$  in the melt was realized by adding ultrapure elemental vanadium (99.9995%) or vanadium pentoxide  $V_2O_5$  (99.995%) to the GaAs melt. The use of  $V_2O_5$  was motivated by the speculation that vanadium-oxygen complexes could be responsible for deep levels in GaAs.<sup>6,7</sup>

Some of the crystals were additionally doped with either shallow donors (Se, Si) or shallow acceptors (Zn) in order to vary the Fermi-level position across the entire band gap.

A key element in this study was the investigation of low-temperature solution-grown *n*-type V-doped crystals prepared by liquid-phase electroepitaxy (LPEE)<sup>18</sup>. Without intentional doping, this technique yields electron-trap-free GaAs crystals,<sup>19</sup> providing a unique means for the unambiguous identification of levels introduced by vanadium.

In our investigation we also employed melt-grown inverted thermal conversion (ITC) V-doped GaAs crystals.<sup>20</sup> This new type of GaAs crystal contains virtually no native midgap levels (EL2), allowing the study of V-related optical-absorption spectra without interference from the well-known EL2 absorption.

Hall-effect measurements were conducted by using the standard Van der Pauw configuration. Ohmic contacts were fabricated by using an In/Sn alloy for *n*-type samples and an In/Zn alloy for *p*-type samples. Typically, measurements were carried out at 300 and 77 K. For several samples, carrier concentration as a function of temperature was measured over the range of 170–465 K.

The features of our transient capacitance system pertinent to this study include (a) precise temperature control and monitoring in the range 15–420 K, (b) direct emission-rate measurements over a range  $10^{-3}$ – $10^4 \text{ s}^{-1}$  from capacitance relaxation recorded with a signal averager, (c) stan-

<sup>a)</sup> On leave from the Institute of Experimental Physics, Warsaw University, Warsaw, Poland.

standard deep-level transient spectroscopy (DLTS) mode operation with the use of a boxcar averager, and (d) optical deep-level spectroscopy (ODLTS) operation with the use of 1.06- $\mu\text{m}$  excitation from a YAG laser. Schottky diodes were fabricated by evaporating Au onto  $n$ -type samples and Al onto  $p$ -type material.

Optical-absorption measurements were performed at 300, 77, and 5 K on a Cary model 17 spectrophotometer using a helium-gas-flow cryostat. Samples were typically from 0.5 to 1.0 cm thick. All of the absorption measurements performed at 5 K were preceded by a period of white light illumination in order to photoquench the well-known absorption due to EL2. All of the photoconductivity measurements were performed at 77 K on a simple LiF prism-based optical system.

### III. EXPERIMENTAL RESULTS AND DISCUSSION

#### A. Hall-effect measurements

Doping with vanadium increased the resistivity of  $n$ -type GaAs and had no effect on the resistivity of  $p$ -type crystals. Standard Hall-effect measurements on low-resistivity  $n$ -type V-doped GaAs crystals yielded low-temperature free-electron mobility ( $\mu$ ) values that were systematically smaller than those obtained at room temperature. Typical results for crystals with free-electron concentrations ( $n$ ) equal to a few times  $10^{16} \text{ cm}^{-3}$  were the following:  $\mu = 2800\text{--}3100 \text{ cm}^2/\text{Vs}$  at 77 K and  $\mu = 3400\text{--}3700 \text{ cm}^2/\text{Vs}$  at 300 K. These results, indicative of a high degree of ionized impurity scattering at low temperature due to the presence of vanadium, can be tentatively explained by assuming that vanadium acts as an acceptor in this material.

From systematic Hall-effect measurements as a function of temperature between 170 and 465 K, the free-carrier concentration ( $n$ ) can be plotted as a function of reciprocal temperature, as shown in Fig. 1. From these data the energy ( $E_A$ ) of a compensating vanadium level was found to be

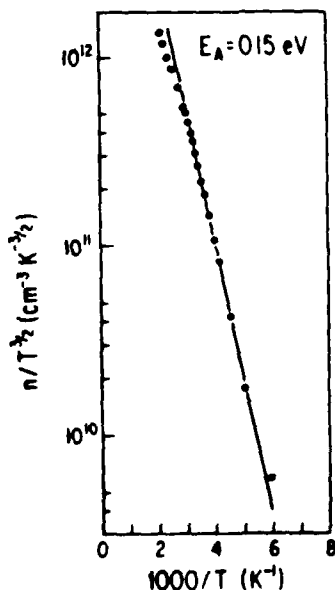


FIG. 1. Activation plot  $n/T^{3/2}$  vs  $1000/T$  of the free-electron concentration in high-resistivity LEC V-doped  $n$ -type GaAs ( $N_V > N_D$ ).

$0.15 \pm 0.01 \text{ eV}$  below the conduction band.<sup>16</sup> In this analysis we have assumed the Hall-scattering factor ( $r_n$ ) to be equal to 1.1 ( $\pm 10\%$ ) throughout the measured temperature range.

Further analysis of the Hall data can provide an estimate of the concentration of vanadium centers by using the charge-balance expression given by Look<sup>21</sup>:

$$n + \frac{N_V}{1 + \Phi_{AC}/n} = N_D^+ - N_A^-,$$

where  $\Phi_{AC} = (g_{A0}/g_{A1})N_C T^{3/2} e^{-E_A/kT}$  is a "modified" density-of-states function,  $N_C = 2(2\pi m_e^* k)^{3/2}/h^3 = 8.1 \times 10^{13} \text{ cm}^{-3} \text{ K}^{-3/2}$ ,  $N_V$  is the concentration of vanadium-related centers (assumed to be acceptors in this case),  $g_{A0}$  ( $g_{A1}$ ) is the degeneracy of the unoccupied (occupied) state,  $E_A$  is the level energy measured from the bottom of the conduction band (a positive value),  $n$  is the concentration of free electrons, and  $N_D^+$  and  $N_A^-$  are the concentrations of all ionized donors and acceptors (excluding vanadium), respectively. By curve fitting to the  $n(T)$  data, the concentration of vanadium-related centers ( $N_V$ ) can be estimated to be a few times  $10^{16} \text{ cm}^{-3}$  with an occupation fraction of these centers ( $N_V^-/N_V$ ) between 0.4 and 0.6 at 200 K. With use of the free-electron mobility values in compensated GaAs calculated by Walukiewicz *et al.*<sup>22,23</sup> for 77 and 300 K, the degree of shallow-donor compensation in these crystals ( $N_D^+/N_D$ ) falls between 0.5 and 0.8. Combination of these results gives an upper limit for the concentration of vanadium-related acceptors of about  $5 \times 10^{16} \text{ cm}^{-3}$ .

#### B. DLTS measurements

DLTS and capacitance transient experiments were performed on low-resistivity GaAs:V,Se crystals where the selenium-donor concentration ( $N_D$ ) exceeded the concentration of vanadium-related centers. The free-electron concentration in these crystals is weakly dependent on temperature, making it possible to carry out capacitance transient measurements to well below 77 K. Typical DLTS spectra in the range 100–440 K for a reference LEC GaAs:Se crystal, a LEC GaAs:V,Se crystal, a reference HB GaAs:Si crystal, and a HB GaAs:V,Se crystal are shown in Figs. 2(a), 2(b) and Figs. 3(a), 3(b), respectively. The dominant mid-gap level EL2 is clearly visible in all LEC and HB spectra at about 390 K. No other midgap levels could be detected. However, in V-doped crystals a new peak at about 100 K appears, indicating the presence of a new electron trap. In the  $n$ -type LPEE GaAs:V crystals this same electron trap is present, as shown in Fig. 2(c). These crystals are electron-trap free without vanadium doping; thus the presence of this new electron trap in this material provides proof that it is related to vanadium.

Capacitance transients caused by electron emission from this trap were measured as a function of temperature in order to obtain values of the activation energy and electron-capture cross section. From the thermal activation plot of the emission rate ( $T^2 e_n^{-1}$  vs  $1000/T$ ), which is presented in Fig. 4, we have found<sup>15</sup> an activation energy for this vanadium-related trap of  $0.15 \pm 0.01 \text{ eV}$  and an electron-capture cross section  $\sigma_n$  of about  $2 \times 10^{-14} \text{ cm}^2$ . We were unable to

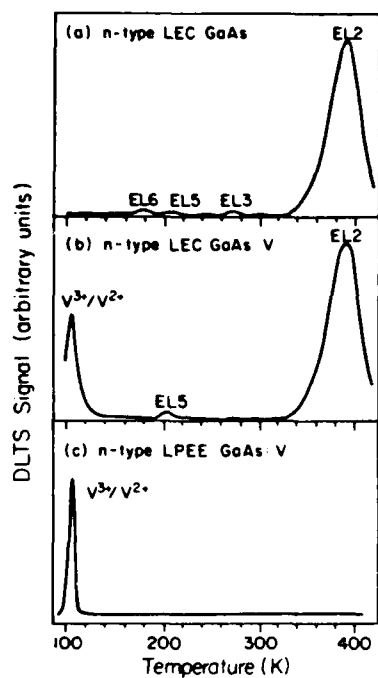


FIG. 2. DLTS spectra of (a) *n*-type LEC GaAs, (b) low-resistivity V-doped LEC GaAs ( $N_V < N_D$ ), and (c) V-doped *n*-type LPEE GaAs.  $t_1/t_2 = 5$  ms/10 ms.

measure the temperature dependence of this cross section. However, for the case of Ti-doped GaAs having an acceptor level of  $E_c - 0.23$  eV,<sup>24</sup> the activation energy of the electron-capture cross section was found to be smaller than 0.01 eV,

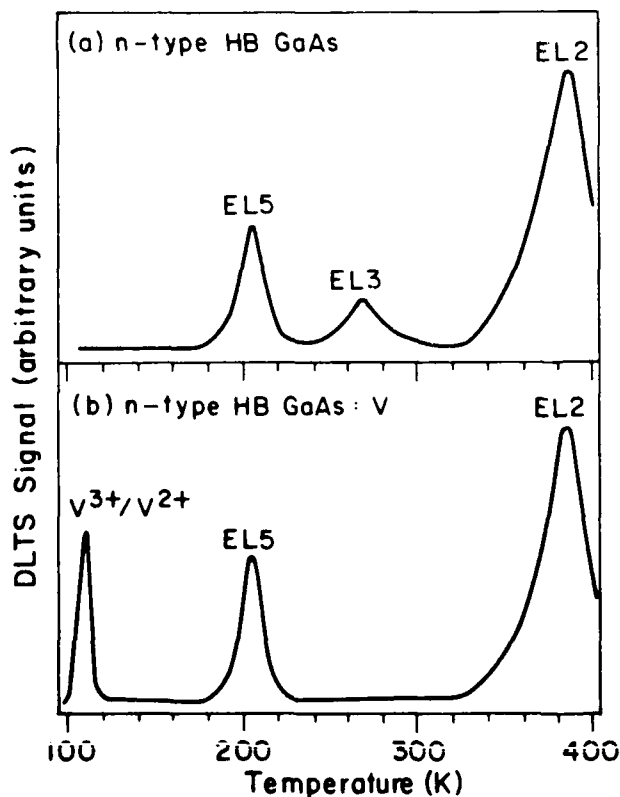


FIG. 3. DLTS spectra of (a) *n*-type HB GaAs and (b) low-resistivity V-doped HB GaAs ( $N_V < N_D$ ).  $t_1/t_2 = 5$  ms/10 ms.

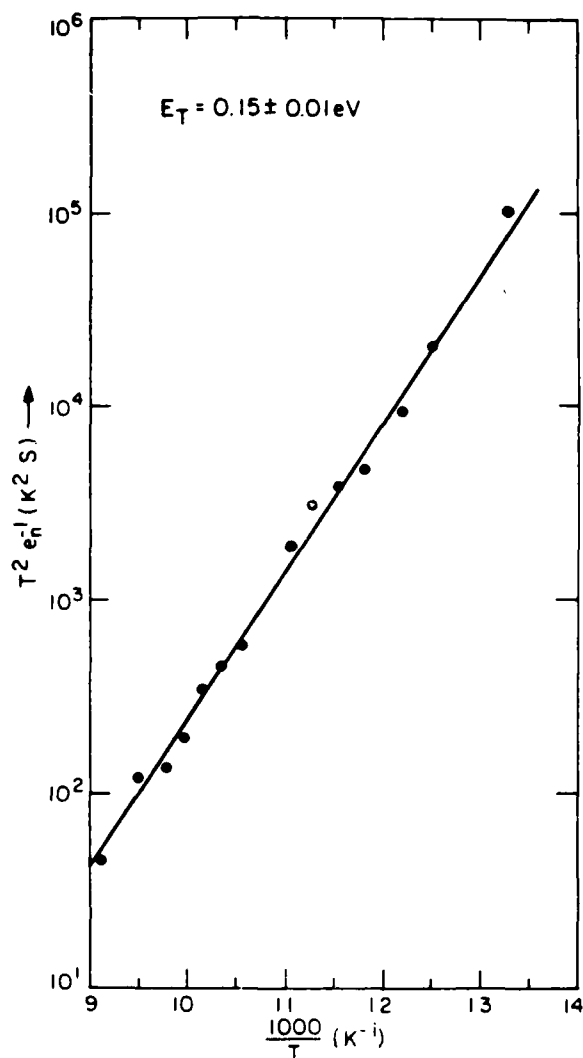


FIG. 4. Emission-rate thermal activation plot  $T^2 e_n^{-1}$  vs  $1000/T$  for V-related electron trap in LEC GaAs.

i.e., our experimental error. Thus, taking into account the agreement between the DLTS and Hall-effect data concerning the level energy, we can assume that the activation energy for electron capture for vanadium is also negligible.

The concentration of vanadium centers calculated from the DLTS data was found to be approximately  $10^{16}$  cm<sup>-3</sup>, in agreement with the value obtained from Hall measurements.

DLTS measurements on *p*-type V-doped GaAs did not reveal any hole trap that could be related to vanadium. Typical DLTS spectra in the range 100–440 K for a reference HB GaAs:Zn crystal and a HB GaAs:V,Zn crystal are shown in Figs. 5(a) and 5(b), respectively. In addition, optical DLTS measurements on *n*-type crystals did not show any minority carrier traps that could be related to vanadium.

In view of the results presented thus far, several conclusions regarding the behavior of vanadium in GaAs can be drawn. Regardless of the dopant form (V or V<sub>2</sub>O<sub>3</sub>), crucible material (SiO<sub>2</sub> or PBN), or growth technique (LEC, HB, or LPEE), vanadium introduces one electron trap into the en-

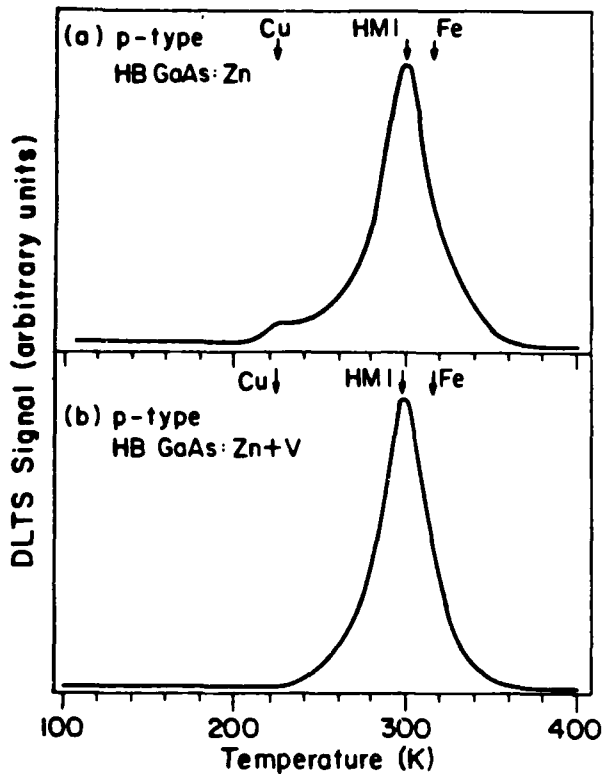


FIG. 5. DLTS spectra of (a) *p*-type HB GaAs and (b) V-doped HB GaAs.  $t_1/t_2 = 5 \text{ ms}/10 \text{ ms}$ .

ergy gap at 0.15 eV below the bottom of the conduction band. No evidence of any midgap level related to vanadium was found, which directly draws into question the utility of vanadium in producing semi-insulating GaAs. The identification of this 0.15-eV vanadium level as an acceptor will be more fully discussed in the following section.

It should be noted that results obtained in some other laboratories did indicate the presence of a vanadium-related acceptor level in the vicinity of the conduction band edge. Thus Clerjaud *et al.*<sup>12</sup> reported electron traps at  $E_c - 0.14 \text{ eV}$  and  $E_c - 0.23 \text{ eV}$  from DLTS measurements of HB GaAs:V, while Ulrici *et al.*<sup>10</sup> reported an acceptor level in LEC GaAs:V at  $E_c - 0.14 \text{ eV}$ . We think that the levels reported at  $E_c - 0.14 \text{ eV}$  are undoubtedly related to vanadium, with the difference between our results and those quoted above lying within the experimental error.

### C. Absorption and photoconductivity spectra

Having identified the level at  $E_c - 0.15 \text{ eV}$  as being introduced by vanadium, we employed optical measurements to obtain information concerning its microscopic nature.

Optical-absorption measurements were performed on both *n*- and *p*-type, V-doped GaAs crystals. In this way, spectra were obtained for Fermi-level positions spanning the entire energy gap. The absorption spectra obtained fell into two primary groups:

(a) For all high-resistivity GaAs:V crystals and *p*-type GaAs:V, Zn crystals (independent of the zinc-doping level),

a characteristic double-peak absorption band was observed between 1.0 and 1.2 eV, preceded at 5 K by a weak zero-phonon line (ZPL) at 1.008 eV and a single absorption line at 0.909 eV. An additional absorption band starting at about 1.35 eV and superimposed on the fundamental absorption edge was also observed. All of these absorption features are shown in Fig. 6(a).

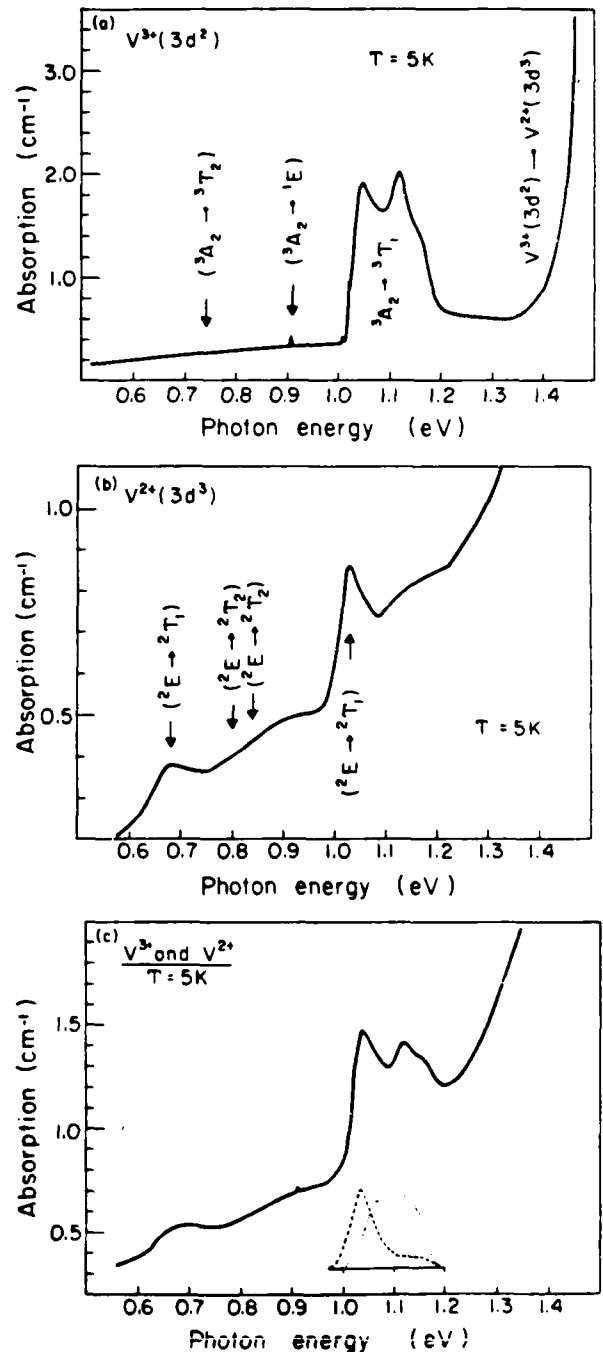


FIG. 6. Optical-absorption spectra of (a) *p*-type and high-resistivity, (b) *n*-type ( $N_V < N_D$ ), and (c) *n*-type ( $N_V > N_D$ ) V-doped GaAs obtained at 5 K. In (a) and (b) assignments of vanadium intracenter transitions according to Ref. 25 are indicated. The inset of (c) shows the relative contribution of the  $V^{2+}$  and  $V^{3+}$  charge states.

(b) For  $n$ -type GaAs:V,Se, heavily doped with selenium ( $N_D > 10^{17} \text{ cm}^{-3}$ ), two absorption bands at 0.68 eV and 1.03 eV without any ZPL were observed, as shown in Fig. 6(b). These bands are superimposed on an absorption background that begins at about 0.3 eV.

For lightly doped  $n$ -type GaAs:V crystals, a mixed absorption spectrum, composed of both (a) and (b)-type absorption features, was observed. Figure 6(c) shows an example of such a mixed absorption spectrum.

The nature of the characteristic absorption band shown in Fig. 6(a) has already been studied and is discussed in detail in the review paper by Clerjaud.<sup>1</sup> This band constitutes an intracenter transition within neutral, substitutional [ $V^{3+}(3d^2)$ ] vanadium between the ground  $^3A_2$  and the excited  $^3T_1$  state. Furthermore, the luminescence spectrum<sup>1</sup> (ZPLs at 0.74 eV), involving the excited  $^3T_2$  and ground  $^3A_2$  states of this  $V^{3+}(3d^2)$  configuration, was also observed in these same samples.<sup>26</sup> Therefore, the vanadium in all of our  $p$ -type and high-resistivity  $n$ -type crystals is in the neutral  $V^{3+}(3d^2)$  charge state. This assignment is further supported by the results of Clerjaud *et al.*<sup>12</sup> who correlated observation of the EPR spectrum of the neutral  $V^{3+}(3d^2)$  with the absorption spectrum in Fig. 6(a).

The absorption line at 0.909 eV in Fig. 6(a) has also been observed by Clerjaud *et al.*<sup>12</sup> and recently interpreted by Caldas *et al.*<sup>25</sup> as being due to the  $^3A_2 \rightarrow ^1E$  spin-forbidden transition of the  $V^{3+}(3d^2)$  charge state.

Figure 6(a) also shows an absorption band starting at 1.35 eV whose intensity correlated with that of the main  $V^{3+}$  intracenter absorption. This result is in agreement with the existing assignment<sup>10,12</sup> of this absorption to the optical transition:

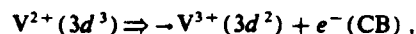


The second type of absorption spectrum shown in Fig. 6(b) is, in our opinion, due to intracenter transitions of the singly ionized  $V^{2+}(3d^3)$  charge state. This spectrum is observed in all low-resistivity  $n$ -type GaAs:V crystals, and its intensity follows that of the DLTS vanadium peak. Furthermore, Fig. 6(c) illustrates the smooth transition between the two different vanadium spectra when the Fermi level is located at the  $E_c - 0.15$ -eV vanadium level. The band at 1.03 eV had been observed by Clerjaud *et al.*<sup>12</sup> and interpreted in terms of the  $V^{2+}(3d^3)$  intracenter transition. However, they did not observe the band at 0.68 eV because of a rising low-energy absorption background. Ulrici *et al.*<sup>10</sup> did observe both of these bands, but did not interpret them as being connected with the  $V^{2+}(3d^3)$  charge state or correlate them together. We can explain the reason for this omission as the observation by Ulrici *et al.* of a mixed  $V^{3+}$  and  $V^{2+}$  absorption spectrum similar to that presented in Fig. 6(c).

At this time we are unable to make a definite identification of the  $V^{2+}(3d^3)$  electron states responsible for the absorption bands presented in Fig. 6(b), because with the lack of a positive identification of any  $V^{2+}$  EPR spectra, the ground-state symmetry remains uncertain. However, Katayama-Yoshida and Zunger<sup>27</sup> and also Caldas *et al.*<sup>25</sup> have predicted that the ground state of the  $V^{2+}(3d^3)$  configuration in GaAs crystals should be the low-spin  $^2E$  state, rather

than the normally expected (according to Hund's rule) high-spin  $^4T_1$  state. Within this model Caldas *et al.* have interpreted the entire  $V^{2+}(3d^3)$  absorption spectrum, as indicated in Fig. 6(b).

From our identification one can further conclude that the absorption background observed in Figs. 6(b) and 6(c) probably corresponds to the transition



which is complementary to the 1.35-eV absorption observed in the  $V^{3+}$  spectrum.

The results of photoconductivity measurements on these low-resistivity  $n$ -type samples are shown in Fig. 7. The presence of the same two maxima of the  $V^{2+}(3d^3)$  charge state at 0.68 and 1.03 eV in the photoconductivity spectrum is a well-known property of excited states of a many-electron impurity. These states are therefore degenerate with the GaAs conduction band and undergo an autoionization effect,<sup>1,28</sup> making them observable under these experimental conditions.

All of the aforementioned assignments are further supported by electron-paramagnetic-resonance (EPR) measurements of our samples.<sup>29</sup> The characteristic substitutional  $V^{3+}(3d^2)$  spectrum<sup>4</sup> was observed for all  $p$ -type and high-resistivity  $n$ -type V-doped GaAs samples. In the case of samples with the Fermi-level position above the  $E_c - 0.15$ -eV level, no EPR spectrum was found, which can be attributed to the high conductivity of such samples.

To conclude this discussion, we can state unequivocally that the optical and electrical properties of V-doped GaAs are self-consistent. Identification of the substitutional non-complexed-vanadium optical spectra enables us to identify the  $E_c - 0.15$  eV level as the  $V^{3+}(3d^2)/V^{2+}(3d^3)$  single acceptor. Furthermore, the observation of the intracenter

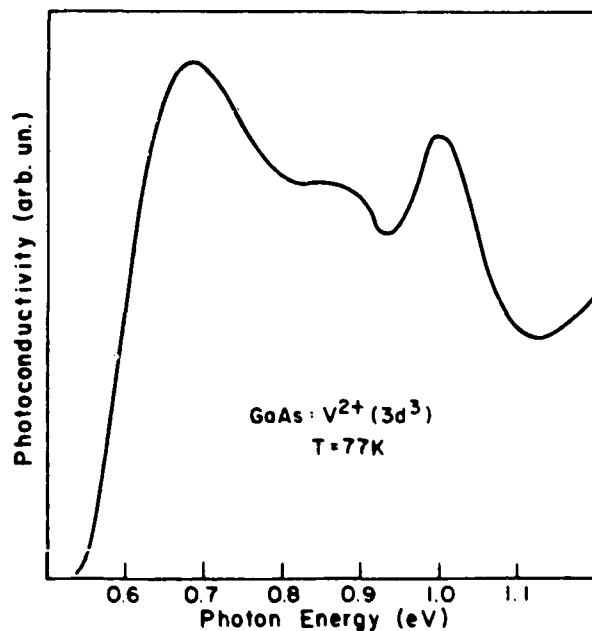


FIG. 7. Photoconductivity spectrum of  $n$ -type V-doped GaAs obtained at 77 K.

$V^{3+}$  absorption spectrum for all positions of the Fermi level between the  $V^{3+}/V^{2+}$  acceptor level and the valence band proves that there is no other substitutional-vanadium level within the GaAs energy gap, i.e., that the  $V^{4+}(3d^1)/V^{3+}(3d^2)$  donor level must be located within the valence band. Figure 8 schematically presents all of the substitutional-vanadium levels in GaAs.

#### D. Calibration of the optical spectra

The DLTS and optical-absorption spectra obtained from low-resistivity V-doped GaAs samples provide the data necessary to calculate the optical-absorption cross sections ( $\sigma$ ) of the  $V^{2+}(3d^3)$  intracenter transitions [Fig. 6(b)]. At liquid-helium temperature their values are the following:

$$\begin{aligned}\sigma(1.03 \text{ eV}) &= \frac{\alpha(1.03 \text{ eV}) - \alpha(0.95 \text{ eV})}{N(\text{DLTS})} \\ &= 3.5 \times 10^{-17} \text{ cm}^2 (\pm 20\%), \\ \sigma(0.68 \text{ eV}) &= \frac{\alpha(0.68 \text{ eV}) - \alpha(0.60 \text{ eV})}{N(\text{DLTS})} \\ &= 1.5 \times 10^{-17} \text{ cm}^2 (\pm 20\%),\end{aligned}$$

where  $\alpha(E)$  is the absorption coefficient for the photon energy  $E$ , and  $N(\text{DLTS})$  is the concentration of vanadium centers obtained from DLTS measurements.

Our as-grown LEC GaAs crystal have a native defect acting as a deep acceptor, which disappears after a standard 850 °C anneal.<sup>30</sup> This native defect provides compensation in as-grown material sufficient to position the Fermi level at or slightly below the 0.15-eV vanadium level, resulting in a  $V^{3+}$  or mixed absorption spectrum; after annealing, only a pure  $V^{2+}$  spectrum is observed. We have used this phenomenon to extend our calibration to the  $V^{3+}(3d^2)$  main intracenter transition. Comparing the as-grown and annealed spectra of the same  $n$ -type V-doped samples, we were able to use the above calibration to find the  $V^{3+}(3d^2)$  absorption cross section at liquid-helium temperature as

$$\begin{aligned}\sigma(1.04 \text{ eV}) &= \frac{\alpha(1.04 \text{ eV}) - \alpha(0.97 \text{ eV})}{N(\text{DLTS})} \\ &= 1 \times 10^{-16} \text{ cm}^2 (\pm 40\%),\end{aligned}$$

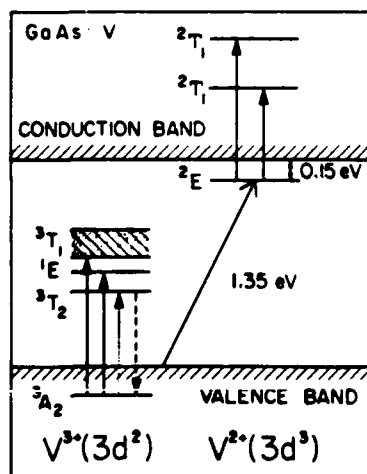


FIG. 8. Energy levels of the  $V^{3+}(3d^2)$  and  $V^{2+}(3d^3)$  charge states in GaAs. Vertical arrows represent intracenter transitions and the slanted arrow represents the charge transfer  $V^{3+}(3d^2) + e^- \Rightarrow V^{2+}(3d^3)$ . The indicated level symmetries have been taken from Ref. 25.

#### E. Theoretical considerations and comparison with other III-V compounds

In addition to all of the technological and experimental studies of V-doped GaAs, some theoretical calculations have also been performed.<sup>25,27</sup> These calculations were not only directed toward an identification of a vanadium spin state (as was mentioned before), but also strove to provide positions of the energy levels within the band gap. The  $V^{3+}/V^{2+}$  acceptor level has been calculated to be at  $E_v + 1.35 \text{ eV}$  (Ref. 25) and  $E_v + 1.34 \text{ eV}$  (Ref. 27), respectively. The  $V^{4+}/V^{3+}$  donor level in both cases has been predicted to be inside the valence band; in one case its position could be estimated as  $-0.03 \text{ eV}$  (Ref. 25) below the top of the valence band. All of these predictions are in a very good agreement with our experimental findings.

Furthermore, based on the findings of Ledebro and Ridley<sup>31</sup> and also of Caldas *et al.*,<sup>32</sup> that the vacuum-referred binding energies (VRBE) of transition-metal impurities remain nearly constant within a given class of semiconducting compounds (i.e., III-V crystals), we can present the available data about substitutional-vanadium levels in the III-V semiconductors. In the case of indium phosphide, the  $V^{4+}(3d^1)/V^{3+}(3d^2)$  donor level has been found at  $E_v + 0.21 \text{ eV}$  (Refs. 33 and 34) or  $E_v + 0.24 \text{ eV}$  (Ref. 35), and the  $V^{3+}(3d^2)/V^{2+}(3d^3)$  acceptor level is proposed by Lambert *et al.*<sup>36</sup> to lie in the conduction band. For  $n$ -type gallium phosphide, the vanadium-acceptor level has only recently been identified at  $E_c - 0.58 \text{ eV}$  (Ref. 37). Measurements on  $p$ -type GaP should reveal the vanadium-donor level as well.

All of these experimental results are presented in Fig. 9 with the use of the electron-affinity data from Ref. 32. One

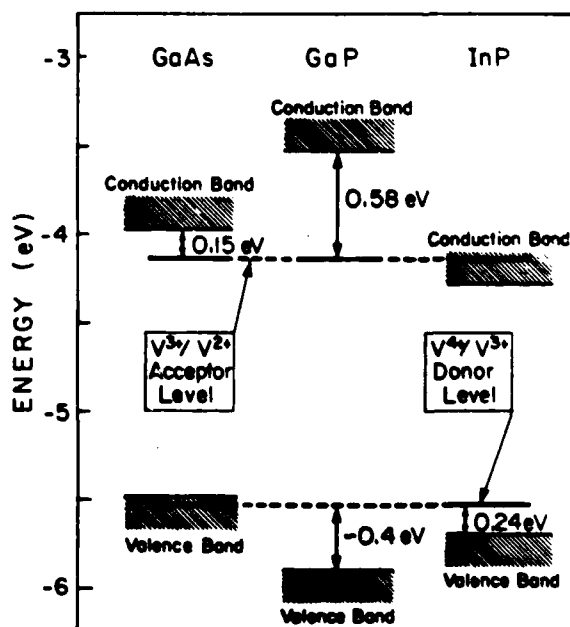


FIG. 9. Vacuum-related binding energies of the vanadium-donor and -acceptor levels in some III-V compounds. The vanadium-donor level in GaP has not yet been observed, but is predicted to lie at  $E_v + 0.4 \text{ eV}$ .

can see excellent agreement between the reported vanadium VRBEs and also predict that the vanadium-donor levels are located at about  $E_v + 0.4$  eV in GaP and very close to the top of the valence band in GaAs.

It is also evident from this figure that none of the substitutional-vanadium levels in GaAs or InP can act as centers for producing SI material.

#### F. Implications for SI GaAs

All of the above experimental and theoretical results prove that the substitutional  $V^{3+}(3d^2)/V^{2+}(3d^3)$  acceptor level at  $E_c - 0.15$  eV is the only vanadium-related level found within the GaAs energy gap. However, several authors have suggested the existence of electrically active vanadium-related complexes in GaAs<sup>5-8,10,37-39</sup> as possibly providing a midgap level. Models invoking a vanadium-oxygen complex<sup>6,7</sup> or a vanadium-arsenic vacancy complex<sup>10,38</sup> have been put forth. We did not detect any optical or electronic evidence of a vanadium-related midgap level in our *n*-type LEC, HB, and LPEE V-doped crystals.

For the case of a vanadium-arsenic vacancy complex model,<sup>10,38</sup> it should be mentioned that although an analogy with a chromium trigonal center  $Cr^{2+}-X$  (see, for example, Ref. 1) is used, there is no experimental evidence (analogous to the known properties of the chromium complex) that such a vanadium complex exists. There is also no definite proof that the acoustic-paramagnetic-resonance (APR) spectra<sup>38</sup> and the thermally detected electron-paramagnetic-resonance (TDEPR) spectra<sup>39</sup> are vanadium related. The reported crystals contain several other transition-metal impurities, and the APR and TDEPR measurements give no information about the concentration of investigated anisotropic centers. Last, the authors of this model<sup>10</sup> failed to grow any SI V-doped material.

During the course of our study, several HB SI V-doped crystals were successfully grown and characterized. We have found, however, that the Fermi-level position in these crystals is controlled by the deep donor EL2, which is present in concentrations greater than that of substitutional vanadium as determined from optical-absorption measurements. Furthermore, the absorption and EPR data from these SI samples are identical to those discussed in Sec. C.

All of these arguments lead quite clearly to the conclusion that vanadium does not play an electronic role in the formulation of SI GaAs. The results do suggest, however, that vanadium could play a more subtle chemical role (e.g., as a gettering agent), thus aiding in the growth of normal EL2-compensated SI material, rather than being directly responsible for its electrical properties. In Table I we have collected all of the published data on the energy levels in V-doped GaAs crystals as of this writing. Comments as to the actual origin of the dominant deep level in each case (e.g.,  $V^{3+}/V^{2+}$  or EL2), in view of the results presented in this study, are also included.

#### IV. CONCLUSIONS

Through the use of DLTS, Hall-effect, and optical-absorption measurements, we have identified the substitutional-vanadium  $V^{3+}/V^{2+}$  acceptor level in GaAs at 0.15 eV

TABLE I. Deep levels observed in V-doped GaAs.

Energy position (eV)	Crystal growth method <sup>a</sup>	Relation to vanadium	Possible origin
$E_c - 0.15^b$	LEC, HB, LPEE	$V^{3+}/V^{2+}$ acceptor	
$E_c - 0.14^c$	LEC	$V^{3+}/V^{2+}$ acceptor	
$E_c - 0.14^d$	HB	$V^{3+}/V^{2+}$ acceptor	
$E_c - 0.22^e$	LEC	not related to V	EL14 or Ti <sup>f</sup>
$E_c - 0.23^d$	HB	not related to V	EL14 or Ti <sup>f</sup>
$E_c - 0.5^g$	MOCVD	not related to V	?
$E_c - 0.77^h$	LEC	not related to V	EL2
$E_v + 0.58^i$	VPE	not related to V	HM1 <sup>j,k</sup>

<sup>a</sup>(LEC) liquid-encapsulated Czochralski, (HB) horizontal Bridgman, (LPEE) liquid-phase electroepitaxy, (MOCVD) metallo-organic chemical vapor deposition, (VPE) vapor-phase epitaxy.

<sup>b</sup>References 15, 16, and this study.

<sup>c</sup>Reference 10.

<sup>d</sup>References 11, 12, and 40.

<sup>e</sup>Reference 9.

<sup>f</sup>Reference 24.

<sup>g</sup>Reference 7.

<sup>h</sup>References 2 and 3.

<sup>i</sup>Reference 6.

<sup>j</sup>J. Lagowski, D. G. Lin, T.-P. Chen, M. Skowronski, and H. C. Gatos, *Appl. Phys. Lett.* **47**, 929 (1985).

<sup>k</sup>J. Osaka, H. Okamoto, and K. Kobayashi, in *Semi-Insulating III-V Materials, Hakone, 1986*, edited by H. Kukimoto and S. Miyazawa (North-Holland/OHMSHA, Tokyo, 1986), p. 421.

below the bottom of the conduction band. The substitutional-vanadium  $V^{4+}/V^{3+}$  donor level was found to be located within the valence band. In addition, no evidence of any midgap level due to vanadium-impurity (defect) complexes was observed. These results confirm the fact that vanadium cannot provide the compensation necessary for producing SI GaAs. The high resistivity of some SI V-doped GaAs crystals can be readily explained by the overwhelming presence of the native defect EL2. We believe that vanadium can, however, play an important chemical role by removing or reacting with residual shallow donors during the growth of high-resistivity material.

#### ACKNOWLEDGMENTS

We are deeply indebted to Dr. T. Bryskiewicz for growing the V-doped LPEE GaAs crystals. We are very grateful to Dr. B. Clerjaud (Université Paris VI) for the EPR measurements of our crystals and many helpful discussions, to Dr. P. W. Yu for the luminescence measurements of our crystals, to Dr. P. Becla for his help in our photoconductivity measurements, and to L. Pawlowicz and F. Dabkowski for growing some of the V-doped LEC GaAs crystals used in this study. We are also grateful to the Air Force Office of Scientific Research and the Office of Naval Research for financial support and the IBM Corporation for C. D. Brandt's graduate fellowship.

<sup>1</sup>For a review, see B. Clerjaud, *J. Phys. C* **18**, 3615 (1985).

<sup>2</sup>A. V. Vasil'ev, G. K. Ippolitova, E. M. Omel'yanovskii, and A. M. Ryskin, *Sov. Phys. Semicond.* **10**, 341 (1976).

<sup>3</sup>V. S. Vavilov and V. A. Morozova, *Sov. Phys. Semicond.* **20**, 226 (1986).

<sup>4</sup>U. Kaufmann, H. Ennen, J. Schneider, R. Worner, J. Weber, and F. Kohl, *Phys. Rev. B* **25**, 5598 (1982).

<sup>5</sup>P. S. Gladkov and K. B. Ozanyan, *J. Phys. C* **18**, L915 (1985).

- <sup>4</sup>H. Terao, H. Sunakawa, K. Obata, and H. Watanabe, in *Semi-Insulating III-V Materials, Eviat, 1982*, edited by S. Makram-Ebeid and B. Tuck (Shiva, Nantwich, England, 1982), p. 54.
- <sup>5</sup>M. Akiyama, Y. Karawada, and K. Kaminiishi, *J. Cryst. Growth* **68**, 39 (1984).
- <sup>6</sup>Y. Kawarada, M. Akiyama, and K. Kaminiishi, in *Semi-Insulating III-V Materials, Hakone, 1986*, edited by H. Kukimoto and S. Miyazawa (North Holland/OHMSHA, Tokyo, 1986), p. 509.
- <sup>7</sup>R. W. Haisty and G. R. Cronin, in *Physics of Semiconductors*, edited by M. Hulin (Dunod, Paris, 1964), p. 1161.
- <sup>8</sup>W. Ulrici, K. Friedland, L. Eaves, and D. P. Halliday, *Phys. Status Solidi B* **131**, 719 (1985).
- <sup>9</sup>A. Mircea-Russel, G. M. Martin, and J. Lowther, *Solid State Commun.* **36**, 171 (1980).
- <sup>10</sup>B. Clerjaud, C. Naud, B. Deveaud, B. Lambert, B. Plot-Chan, G. Bremond, C. Benjeddou, G. Guillot, and A. Nouailhat, *J. Appl. Phys.* **58**, 4207 (1985).
- <sup>11</sup>W. Kutt, D. Bimberg, M. Maier, H. Krautle, F. Kohl, and E. Bauser, *Appl. Phys. Lett.* **44**, 1078 (1984).
- <sup>12</sup>W. Kutt, D. Bimberg, M. Maier, H. Krautle, F. Kohl, and E. Tomzig, *Appl. Phys. Lett.* **46**, 489 (1985).
- <sup>13</sup>C. D. Brandt, A. M. Hennel, L. M. Pawlowicz, F. P. Dabkowski, J. Lagowski, and H. C. Gatos, *Appl. Phys. Lett.* **47**, 607 (1985).
- <sup>14</sup>A. M. Hennel, C. D. Brandt, H. Hsiaw, L. M. Pawlowicz, F. P. Dabkowski, and J. Lagowski, *Gallium Arsenide and Related Compounds 1985*, Institute of Physics Conference Service No. 79 (Hilger, Bristol, 1986), pp. 43-48.
- <sup>15</sup>A. M. Hennel, C. D. Brandt, L. M. Pawlowicz, and K. Y. Ko, in *Semi-Insulating III-V Materials, Hakone, 1986*, edited by H. Kukimoto and S. Miyazawa (North Holland/OHMSHA, Tokyo, 1986), p. 465.
- <sup>16</sup>T. Bryskiewicz, in *Semiconductor Optoelectronics*, edited by M. A. Herman (PWN-Polish Scientific, Warsaw, 1980), pp. 187-212; in *Progress in Crystal Growth and Characterization*, edited by B. Pamplin (Pergamon, Oxford, in press).
- <sup>17</sup>T. Bryskiewicz, C. F. Boucher, Jr., J. Lagowski, and H. C. Gatos, *J. Cryst. Growth* (to be published).
- <sup>18</sup>J. Lagowski, H. C. Gatos, C. H. Kang, M. Skowronski, K. Y. Ko, and D. G. Lin, *Appl. Phys. Lett.* **49**, 892 (1986).
- <sup>19</sup>D. C. Look, in *Semiconductors and Semimetals*, edited by R. K. Willardson and A. C. Beer (Academic, New York, 1983), Vol. 19, p. 75.
- <sup>20</sup>W. Walukiewicz, J. Lagowski, L. Jastrzebski, M. Lichtensteiger, and H. C. Gatos, *J. Appl. Phys.* **50**, 899 (1979).
- <sup>21</sup>W. Walukiewicz, J. Lagowski, and H. C. Gatos, *J. Appl. Phys.* **53**, 769 (1982).
- <sup>22</sup>C. D. Brandt, A. M. Hennel, L. M. Pawlowicz, Y.-T. Wu, T. Bryskiewicz, J. Lagowski, and H. C. Gatos, *Appl. Phys. Lett.* **48**, 1162 (1986).
- <sup>23</sup>M. Caldas, S. K. Figueiredo, and A. Fazzio, *Phys. Rev. B* **33**, 7102 (1986).
- <sup>24</sup>P. W. Yu (private communication).
- <sup>25</sup>H. Katayama-Yoshida and A. Zunger, *Phys. Rev. B* **33**, 2961 (1986).
- <sup>26</sup>See, for example, K. Kocot and J. M. Baranowski, *Phys. Status Solidi B* **81**, 629 (1977); A. P. Radlinski, *Phys. Status Solidi B* **84**, 503 (1977).
- <sup>27</sup>B. Clerjaud (private communication).
- <sup>28</sup>C. D. Brandt (unpublished).
- <sup>29</sup>L. A. Ledebro and B. K. Ridley, *J. Phys. C* **15**, L961 (1982).
- <sup>30</sup>M. J. Caldas, A. Fazzio, and A. Zunger, *Appl. Phys. Lett.* **45**, 671 (1984).
- <sup>31</sup>G. Bremond, A. Nouailhat, G. Guillot, B. Deveaud, B. Lambert, Y. Toudic, B. Clerjaud, and C. Naud, in *Microscopic Identification of Electronic Defects in Semiconductors*, Materials Research Society Symposia Proceedings, edited by N. M. Johnson, S. G. Bishop, and G. D. Watkins. (Materials Research Society, Pittsburgh, 1985), Vol. 46, p. 359.
- <sup>32</sup>B. Deveaud, B. Plot, B. Lambert, G. Bremond, G. Guillot, A. Nouailhat, B. Clerjaud, and C. Naud, *J. Appl. Phys.* **59**, 3126 (1986).
- <sup>33</sup>C. D. Brandt, A. M. Hennel, J. Lagowski, and H. C. Gatos (unpublished).
- <sup>34</sup>B. Lambert, B. Deveaud, Y. Toudic, G. Pelous, J. C. Paris, and G. Grandpierre, *Solid State Commun.* **47**, 337 (1983).
- <sup>35</sup>W. Ulrici, L. Eaves, K. Friedland, D. P. Halliday, and J. Kreibler, in Proceedings of the 14th International Conference on Defects in Semiconductors, Paris, 1986 (to be published).
- <sup>36</sup>V. W. Rampton, M. K. Saker, and W. Ulrici, *J. Phys. C* **19**, 1037 (1986).
- <sup>37</sup>A.-M. Vasson, A. Vasson, C. A. Bates, and A. F. Labadz, *J. Phys. C* **17**, L837 (1984).
- <sup>38</sup>E. Litty, P. Leyral, S. Loualiche, A. Nouailhat, G. Guillot, and M. Lannoo, *Physica B* **117/118**, 182 (1983).

## LPEE Growth and Characterization of $\text{In}_{1-x}\text{Ga}_x\text{As}$ Bulk Crystals

T. Bryskiewicz,\* M. Bugajski,\*\* B. Bryskiewicz, J. Lagowski and H.C. Gatos

Massachusetts Institute of Technology, Cambridge, MA 02139, USA

**ABSTRACT:** A novel procedure for liquid phase electroepitaxial (LPEE) growth of highly uniform multicomponent bulk crystals has been developed and successfully applied to the growth of high quality bulk  $\text{In}_{1-x}\text{Ga}_x\text{As}$  crystals.  $\text{In}_{1-x}\text{Ga}_x\text{As}$  ingots 14 mm in diameter and up to 3 mm thick were grown on (100)  $\text{InP}^x$  substrates. In terms of homogeneity, electrical characteristics, and defect structure they are comparable to high quality thin LPE layers.

### 1. INTRODUCTION

Liquid phase electroepitaxy is a solution growth technique in which the growth process is induced and sustained solely by passing a direct electric current across the solution-substrate interface while the temperature of the overall system is maintained constant (Bryskiewicz, 1986 and references therein). It has been found that after initial stages of growth the solute electrotransport towards the interface becomes the dominant driving force for the growth (Bryskiewicz 1978, Jastrzebski et al 1978, Bryskiewicz et al 1980). Therefore, within a few minutes after an electric current is turned on the growth proceeds under isothermal and steady-state conditions. These features of electroepitaxy have proven (both experimentally and theoretically) to be uniquely suited for the growth of ternary and quaternary semiconductor compounds with constant composition (Daniele 1981, Bryskiewicz et al 1980).  $\text{Ga}_{1-x}\text{Al}_x\text{As}$  wafers as thick as 600  $\mu\text{m}$  (Daniele et al 1981),  $\text{GaAs}_{1-x}\text{Sb}_x$  (Birýulin et al 1983),  $\text{In}_{1-x}\text{Ga}_x\text{P}$  (Daniele et al 1983), and  $\text{Hg}_x\text{Cd}_{1-x}\text{Te}$  (Vanier et al 1980) epilayers up to 200  $\mu\text{m}$ , 120  $\mu\text{m}$ , and 500  $\mu\text{m}$ , respectively, grown by LPEE showed a remarkable uniformity of composition, varying by  $\Delta x=0.01-0.03$  over their entire thickness. However, the growth procedures proposed thus far (Daniele et al 1981, Nakajima 1987) are suitable for the growth of uniform wafers a few hundred microns thick.

In this paper a novel procedure, useful for electroepitaxial growth of bulk crystals (several millimeters thick) of ternary and quaternary semiconductors is proposed. This novel procedure is successfully applied to the growth of high quality  $\text{In}_{1-x}\text{Ga}_x\text{As}$  bulk crystals.

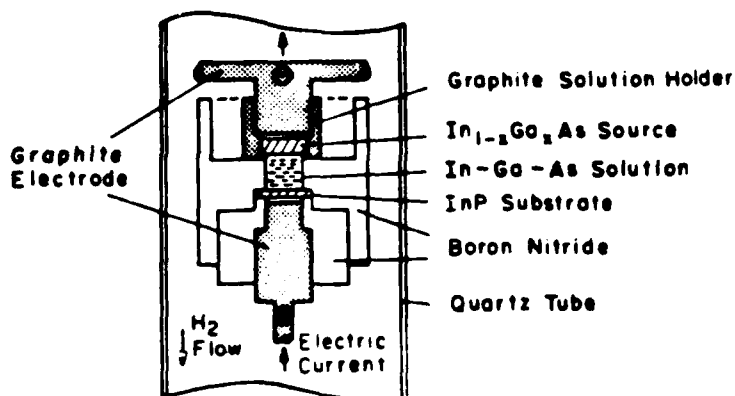
### 2. NOVEL LPEE GROWTH PROCEDURE

The growth of highly uniform  $\text{In}_{1-x}\text{Ga}_x\text{As}$  bulk crystals was carried out in a novel vertical LPEE apparatus (Bryskiewicz et al 1987a), employed recently

\*On leave from Microgravity Research Associates, Inc., Midland, TX 79701, USA.

\*\*On leave from Institute of Electron Technology, 02-668 Warsaw, Poland.

to the growth of epitaxial quality GaAs bulk crystals (Bryskiewicz et al 1987b). A schematic diagram of the growth cell used in our growth experiments is shown in Fig. 1. During electroepitaxial growth solution is



contacted by the substrate at the bottom and the source material at the top. Thus, the crystallizing material driven by the electric current is deposited onto the substrate while the solution is being continuously saturated with the source material. A very important characteristic of the growth cell seen in Fig. 1 is the shape of a graphite source

Fig. 1. Schematic diagram of the growth cell used for LPEE growth of  $\text{In}_{1-x}\text{Ga}_x\text{As}$  bulk crystals.

holder which allows the current to bypass the source material. This results in a minimization of the Joule heating for an arbitrary form (monocrystal, polycrystal, or chunks) of the source material. The requirements for the source are thus limited to the compositional homogeneity and the chemical composition fitted to the composition of the crystal to be grown. In order to achieve these source characteristics, a procedure for the preparation of a macroscopically homogeneous source material had to be developed.

In this study the source material required for the growth of highly uniform  $\text{In}_{1-x}\text{Ga}_x\text{As}$  bulk crystals was prepared in a sealed quartz ampoule evacuated to  $10^{-6}$  Tr. The inner wall of the quartz ampoule was covered with a pyrolytic carbon in order to prevent wetting. A semiconductor grade InAs-GaAs quasibinary mixture and a small amount of a high purity arsenic were sealed in the ampoule, heated up to about 20-30°C above the liquidus temperature and kept molten for one hour. High compositional homogeneity of the  $\text{In}_{1-x}\text{Ga}_x\text{As}$  source material was assured by rapid cooling of the ampoule.  $\text{In}_{1-x}\text{Ga}_x\text{As}$  bulk crystals with compositions between  $x=0.46$  and  $x=0.48$  were grown at 650°C on (100)-oriented, Sn-doped InP substrates. The grown ingots were 14 mm in diameter and up to 3 mm thick, i.e., suitable for slicing up to five wafers.

### 3. CRYSTAL CHARACTERIZATION

A microphotograph of the etch pits revealed on the (100)-oriented InP substrate and on the  $\text{In}_{0.52}\text{Ga}_{0.48}\text{As}$  bulk crystal is seen in Fig. 2. Although the dislocation loops generation process is very likely to occur in this case near the surface, we did not observe any significant increase in the etch pit density between the InP substrate ( $\text{EPD} \sim 5-2 \times 10^5 \text{cm}^{-2}$ ) and  $\text{In}_{1-x}\text{Ga}_x\text{As}$  crystals.

Electrical parameters of the  $\text{In}_{1-x}\text{Ga}_x\text{As}$  bulk crystals grown from unbaked In-rich solutions are shown in Table I. It is expected that the free electron concentration in the low  $10^{16} \text{cm}^{-3}$  range can be reduced considerably by using higher purity solution components and/or by baking the solution prior to each run (Bhattacharya et al 1983). The 300°K mobility as high as 8000  $\text{cm}^2/\text{Vs}$  and the 77°K mobility of about 13,000  $\text{cm}^2/\text{Vs}$  is

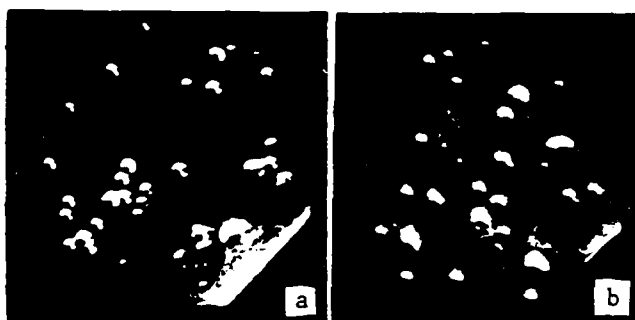


Fig. 2. Optical micrographs showing the typical etch pit pattern observed on (a) (100)-oriented InP substrate; (b)  $\text{In}_{0.52}\text{Ga}_{0.48}\text{As}$  bulk crystal.

quite remarkable for the  $10^{16}\text{cm}^{-3}$  free carrier concentration. These mobility values suggest low compensation and high homogeneity and structural perfection of the  $\text{In}_{1-x}\text{Ga}_x\text{As}$  ingots.

Table I. Electrical characteristics of LPEE  $\text{In}_{1-x}\text{Ga}_x\text{As}$  bulk crystals.

Composition (at.%)	Conductivity Type	Carrier Concentration ( $\text{cm}^{-3}$ )		Mobility ( $\text{cm}^2/\text{Vs}$ )	
		300°K	77°K	300°K	77°K
46	n	$2.7 \times 10^{16}$	$2.4 \times 10^{16}$	6240	13620
47	n	$4.5 \times 10^{16}$	$4.1 \times 10^{16}$	7780	11750
48	n	$4.6 \times 10^{16}$	$4.0 \times 10^{16}$	7640	13140

In addition, DLTS measurements did not reveal any measurable electron traps in these crystals.

Structural perfection as well as high compositional homogeneity of the  $\text{In}_{1-x}\text{Ga}_x\text{As}$  bulk crystals, comparable in quality with thin LPE layers, is documented by a high resolution photoluminescence (PL) spectrum shown in Fig. 3. This spectrum was recorded at 5°K for a nominally undoped n-type

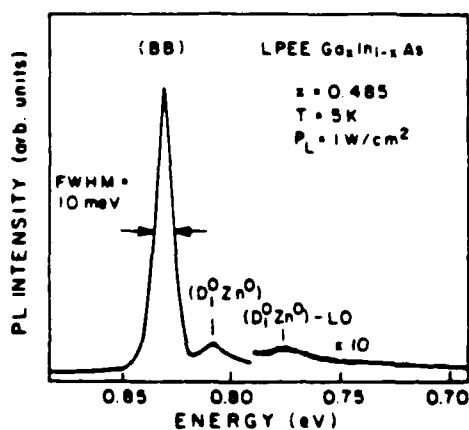


Fig. 3. 5°K PL spectrum of n-type  $\text{In}_{0.52}\text{Ga}_{0.48}\text{As}$  grown on (100) InP substrate;  $n = 4 \times 10^{16}\text{cm}^{-3}$ .

LPEE  $\text{Ga}_{0.52}\text{Ga}_{0.48}\text{As}$  crystal. The dominant line at 0.8303 eV corresponds to the band-to-band transitions (BB). The above assignment was made on the basis of the line shape and the luminescence intensity vs. excitation density dependence (which appeared to be nearly quadratic). As seen in Fig. 3, the full width at half maximum (FWHM) of the (BB) line is equal to 10 meV. This value can be understood in terms of alloy broadening

due to the random distribution of the In and Ga cations. From the model developed for  $\text{Al}_x\text{Ga}_{1-x}\text{As}$  (Schubert et al 1984) the alloy broadening of the BB transitions in  $\text{In}_{1-x}\text{Ga}_x\text{As}$  has been estimated to be in the 9.2-13.7 meV range. The spread in the calculated FWHMs results mainly from the uncertainties of the values of the heavy hole mass and band discontinuity at the  $\text{In}_{1-x}\text{Ga}_x\text{As}/\text{InP}$  heterointerface. Nevertheless, an overall agreement between theory and experiment is satisfactory.

The second line in Fig. 3 located 20.4 meV below the (BB) peak is due to the presence of the residual Zn acceptor, and it corresponds to the donor-

acceptor (DA) type of transitions. The binding energy  $E_A$  of the Zn acceptor estimated from the line position in different samples is  $E_A = 20.6-21.5$  meV, in close agreement with  $E_A = 22 \pm 1$  meV reported by Goetz et al (1983).

The measurements of the (BB) peak position were used to determine the compositional variations vs. a distance from the substrate and along the crystal surface. The results are shown in Fig. 4a and b, respectively. An excellent compositional homogeneity of the  $\text{In}_{1-x}\text{Ga}_x\text{As}$  ingots, both perpendicular and parallel to the growth direction, is evident. In both cases the composition fluctuations do not exceed 1%.

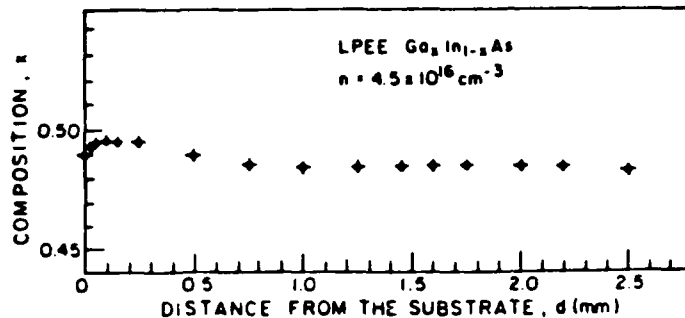
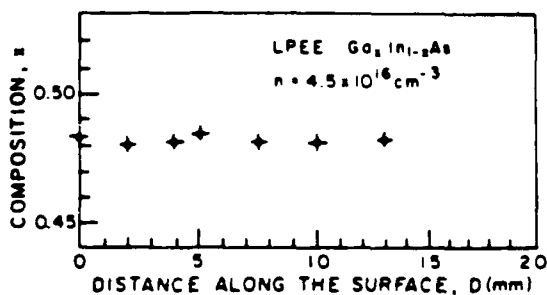


Fig. 4. Composition profile of  $\text{In}_{.52}\text{Ga}_{.48}\text{As}$  obtained from PL measurements:  
(a) along the growth direction



(b) perpendicular to the growth direction.

The authors are grateful to Microgravity Research Associates, Inc., and to the Air Force Office of Scientific Research for financial support.

#### 4. REFERENCES

- Bhattacharya P K, Rao M V and Tsai M-J 1983 J. Appl. Phys. 54, 5096  
 Biryulin Y F, Golubev L V, Novikov S V and Shmartsev Yu V 1983 Sov. Tech. Phys. 9, 68 (Pis'ma Zh. Tekh. Fiz. 9, 155)  
 Bryskiewicz T 1978 J. Cryst. Growth 43, 567  
 Bryskiewicz T, Lagowski J and Gatos H C 1980 J. Appl. Phys. 51, 988  
 Bryskiewicz T 1986 Prog. Crystal Growth and Charact. 12, 29 (Pergamon)  
 Bryskiewicz T, Boucher Jr C F, Lagowski J and Gatos H C 1987a J. Cryst. Growth 82, 279  
 Bryskiewicz T, Bugajski M, Lagowski J and Gatos H C 1987b J. Cryst. Growth (to be published)  
 Daniele J J and Hebling A J 1981 J. Appl. Phys. 52, 4325  
 Daniele J J and Lewis A 1983 J. Electron. Mat. 12, 1015  
 Goetz K H, Rimberg D, Jurgensen H, Selders J, Solomonov A V, Glinski G F and Razeghi M 1983 J. Appl. Phys. 54, 4543  
 Jastrzebski L, Lagowski J, Gatos H C and Witt A F 1978 J. Appl. Phys. 49, 5909; 50, 7269 (1979)  
 Nakajima K 1987 J. Appl. Phys. 61, 4626  
 Schubert E F, Gobel E O, Horikoshi Y, Ploog K and Queisser H J 1984 Phys. Rev. B 30, 813  
 Vanier P A, Pollak F H and Raccah P M 1980 J. Electron. Mat. 9, 153

# Arsenic Ambient Conditions Preventing Surface Degradation of GaAs during Capless Annealing at High Temperatures

C. H. Kang, K. Kondo,<sup>1</sup> J. Logowski, and H. C. Gatos\*

Massachusetts Institute of Technology, Cambridge, Massachusetts 02139

## ABSTRACT

Changes in surface morphology and composition caused by capless annealing of GaAs were studied as a function of annealing temperature,  $T_{\text{GaAs}}$ , and the ambient arsenic pressure controlled by the temperature,  $T_{\text{As}}$ , of an arsenic source in the annealing ampul. It was established that any degradation of the GaAs surface morphology could be completely prevented providing that  $T_{\text{As}} [^{\circ}\text{C}] \geq 0.315 T_{\text{GaAs}} [^{\circ}\text{C}] + 227$ . This empirical relationship is valid up to the melting point temperature of GaAs (1238°C) and it may be useful in some device processing steps.

Annealing at elevated temperature is a key process step in the fabrication of GaAs integrated circuits. The temperatures between 800° and 900°C used for activation of implants are well above the congruent evaporation point (about 640°C) (1). Thus, a preferential loss of arsenic takes place during annealing. In order to prevent structural and compositional degradation of the surfaces, various capping techniques have been developed which employ deposited protective films ( $\text{Si}_3\text{N}_4$ ,  $\text{SiO}_2$ ,  $\text{Al}_2\text{O}_3$ ). Generation of defects during the film deposition and/or excessive interface stresses are common disadvantages of this approach (2). An alternative solution involves capless annealing in an ambient containing arsenic vapor at a partial pressure high enough to prevent decomposition of GaAs surfaces. Various sources of arsenic vapor have been proposed, i.e., GaAs powder or wafers (3, 4), "melt-controlled" ambients (5-7), InAs (8, 9), flowing  $\text{AsH}_3$  (10-12), or a gas enriched with arsenic (13, 14); however, no systematic quantitative study has been made on the behavior of the surface morphology as a function of the arsenic vapor pressure.

In the present study elemental arsenic was employed as a source material supplying arsenic vapor to the annealing ambient. Surfaces of GaAs crystals were examined (prior to and after annealing) by optical and electron microscopes, electron microprobe, and x-ray photoelectron spectroscopy. Experimental conditions were established under which no degradation of the surface morphology and the surface composition took place upon annealing. These conditions are expressed in terms of a relationship between the annealing temperature,  $T_{\text{GaAs}}$ , and the required temperature of the arsenic source,  $T_{\text{As}}$ .

## Experimental Procedures

Annealing experiments were carried out in a closed two-zone apparatus shown schematically in Fig. 1. GaAs samples and elemental arsenic were placed in a closed quartz ampul in the hot and cold zone, respectively. They were separated by a distance of about 40 cm. The volume of the ampul was about 150 cm<sup>3</sup>. The temperature of the arsenic source was precisely controlled in a sodium-filled Inconel heat pipe inserted into a cold zone of the resistance furnace.

GaAs crystals employed in this study were grown by the horizontal Bridgman (HB) and the liquid encapsulated Czochralski (LEC) techniques. Wafers with (100) and (111) surfaces were polished to a mirror-like finish, using a polishing solution containing 1 part of chlorox bleach and 4 parts of  $\text{H}_2\text{O}$ . After polishing, the samples were cleaned in trichloroethylene, acetone, and methanol. They were rinsed in deionized water and etched in concentrated  $\text{H}_2\text{SO}_4$ , and then in a stagnant solution of  $3\text{H}_2\text{SO}_4 + 1\text{H}_2\text{O}_2 + 1\text{H}_2\text{O}$  for 5 min. They were rinsed again in deionized water and then etched in HCl for 5 min to remove any oxide or organic material on the surface. Finally, the specimens were rinsed in deionized water and dried with a stream of nitrogen gas. Elemental

arsenic of 99.9999% purity was cleaned and etched in the same way as the GaAs.

The GaAs samples and arsenic source material were placed at the opposite ends of the high purity quartz ampul, which was precleaned by etching in  $1\text{HF} + 1\text{HNO}_3$ , washing in deionized water, and drying. The ampul was heated at 300°C for 3h under  $5 \times 10^{-7}$  torr vacuum in order to accelerate the removal of residual oxides and adsorbed water. The ampul was then cooled to room temperature and sealed off under vacuum.

The annealing treatment was carried out after loading the sealed ampul into a preheated horizontal two-zone furnace. The annealing temperature was varied from 650° to about 1000°C, while the arsenic source temperature was varied from 400° to 620°C. The annealing time was varied from 30 min to 20h.

The as-annealed GaAs surfaces were examined by Nomarski phase contrast microscopy. X-ray photoelectron spectroscopy (XPS) was used for the determination of the concentration ratio of [As]/[Ga] on the surface. Compositional changes on a microscale were determined by electron probe microanalysis (EPMA). In order to reveal variations on the surface with a high spatial resolution scanning electron microscopy (SEM) was carried out employing surfaces coated with carbon. The SEM apparatus was equipped with an attachment for energy dispersion x-ray analysis.

## Results and Discussions

Surface degradation due to condensation of arsenic — Upon termination of annealing the ampul is cooled down and the arsenic vapor becomes supersaturated. Condensation of arsenic on the GaAs surfaces leads to degradation of surface morphology. This degradation can be especially severe for high arsenic pressures which are

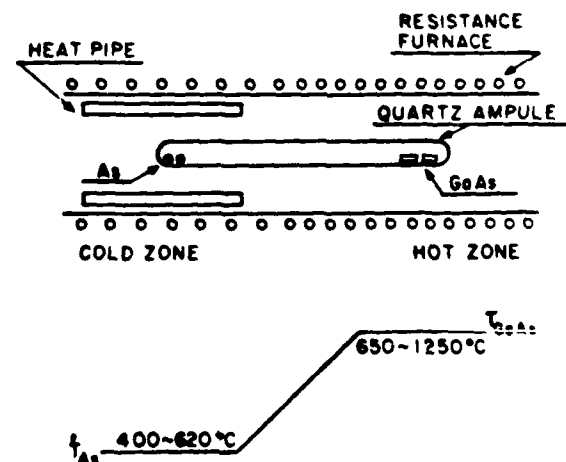


Fig. 1. Two zone apparatus employed for annealing of GaAs and corresponding temperature profile.

\*Electrochemical Society Honorary Member.

<sup>1</sup>Present address: Fujitsu Laboratories, Atsugi, Japan.

required to prevent arsenic loss from the surface during actual annealing.

Experimental results illustrating the detrimental effects of arsenic condensation are shown in Fig. 2, column (a). In this case, after annealing, the whole ampul was quenched in water to room temperature. The samples were then cleaned in concentrated HCl in order to remove arsenic condensed during rapid cooling; HCl does not react with GaAs. The Nomarski photomicrographs shown in Fig. 2 illustrate the roughness of surfaces annealed at different  $T_{As}$ . For low arsenic source temperatures (494° and 510°C) thermal etching of GaAs takes place during annealing (due to preferential evaporation of arsenic), resulting in a poor surface quality. After passing through an optimum of  $T_{As} \sim 521^\circ\text{C}$ , the surface quality degrades again for higher arsenic source temperatures.

As shown in column (b) this surface degradation does not occur if the cooling is carried out so that the ampul end containing the elemental arsenic is quenched prior to quenching the end containing the GaAs; the entire quenching process is completed within a few seconds. Under such conditions most of the arsenic vapor condenses on the inside ampul wall of the arsenic source zone, and the GaAs surfaces are not contaminated with arsenic. During this cooling procedure, no depletion of arsenic from the GaAs surfaces was observed (see below). Photomicrographs shown in column (b) correspond to "as-annealed" surfaces without cleaning in HCl which was used for the surfaces shown in column (a).

**Surface stability range.**—When the detrimental effects of arsenic condensation during postannealing cooling

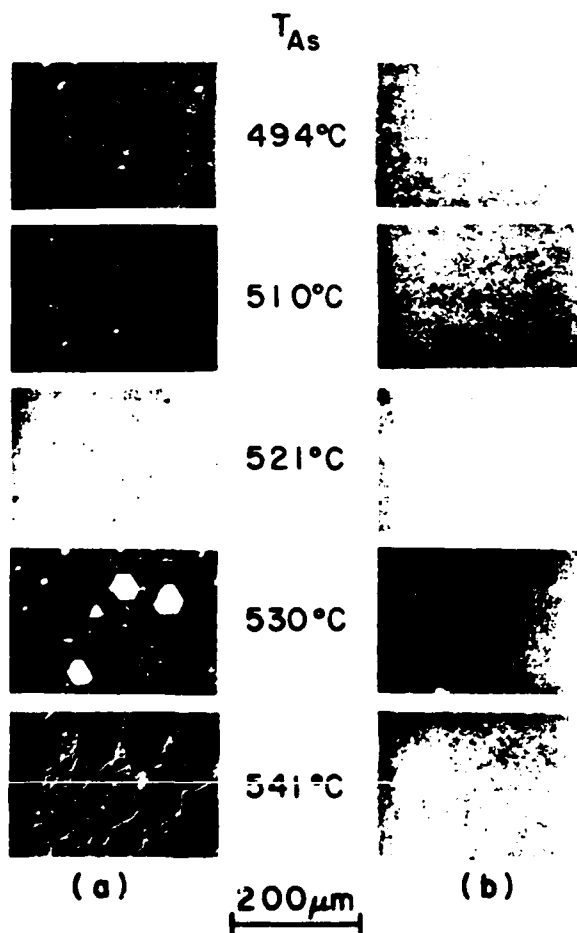


Fig. 2. Photomicrographs of GaAs surfaces after 900°C annealing for 16h with different arsenic source temperatures. Column (a) arsenic source and GaAs were cooled simultaneously; column (b) arsenic source was quenched first.

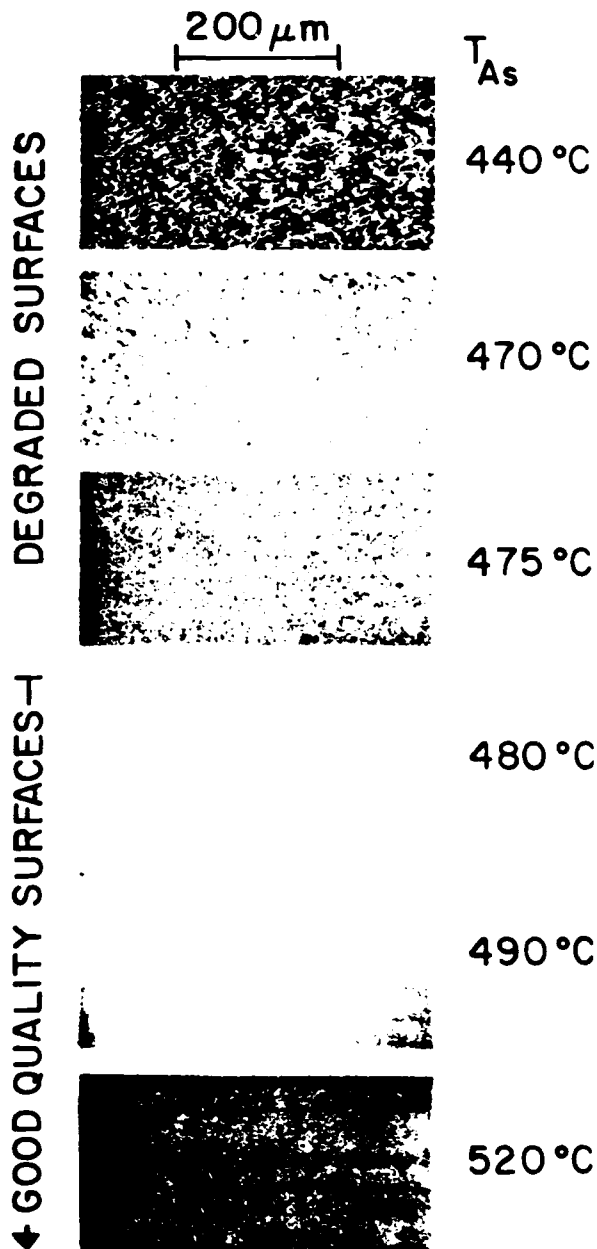


Fig. 3. Nomarski micrographs of surfaces of GaAs annealed at 800°C for 16h with different temperatures of arsenic source. (Arsenic source was quenched first.)

are eliminated, the surface quality remains very good for high arsenic source temperatures. However, deterioration of the surfaces always takes place for low  $T_{As}$  values. Nomarski phase contrast micrographs of GaAs annealed at 800°C for 16h under different  $T_{As}$  values are shown in Fig. 3.  $T_{As}$  of 440°, 470°, and 475°C yielded poor quality surfaces, while  $T_{As} = 480^\circ, 490^\circ,$  and  $520^\circ\text{C}$  yielded surfaces of good quality. We performed a series of such annealing experiments, the results are summarized in Fig. 4 in the form of a pressure-temperature diagram. For each annealing temperature the arsenic source temperatures yielding poor quality surfaces are marked with filled circles, while open circles correspond to good quality surfaces.

The borderline drawn between filled and open circles separates the regions of good and bad surface morphologies. It is of interest to note that the borderline passes through the point  $T_{GaAs} = 1238^\circ\text{C}$  and  $T_{As} = 617^\circ\text{C}$  which corresponds to melting point equilibrium conditions for GaAs with optimum stoichiometry (15).

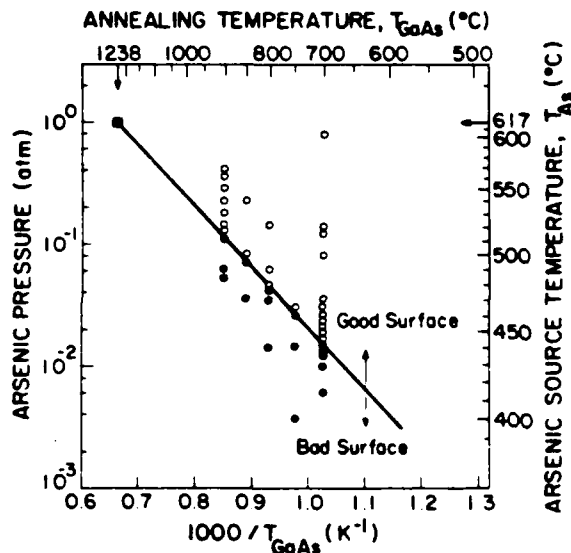


Fig. 4. Pressure-temperature diagram of GaAs showing the arsenic pressures which yield poor (filled circles) and good (open circles) surface morphologies at different annealing temperatures. The equilibrium arsenic pressure value at each arsenic source temperature was adopted from Ref. (16).

Arsenic pressure values given in Fig. 4 represent the total arsenic vapor pressure in equilibrium with solid arsenic at temperature  $T_{As}$ . These values are adopted from Ref. (16).

The borderline separating good and bad morphologies is shown in Fig. 5 in linear  $T_{GaAs}$  and  $T_{As}$  coordinates. The line represents the critical arsenic source temperature,  $T_{As}^*$ , and is described by

$$T_{As}^* [^{\circ}C] = 0.315 T_{GaAs} [^{\circ}C] + 227 \quad (1)$$

Stable surfaces with good morphology are obtained for  $T_{As} \geq T_{As}^*$ , while for lower arsenic source temperatures,  $T_{As} < T_{As}^*$ , surface degradation takes place associated with preferential evaporation of arsenic.

Changes in surface composition.—The XPS spectra shown in Fig. 6 illustrate annealing-induced changes in the surface concentration of gallium and arsenic. Surfaces annealed under low arsenic source temperature

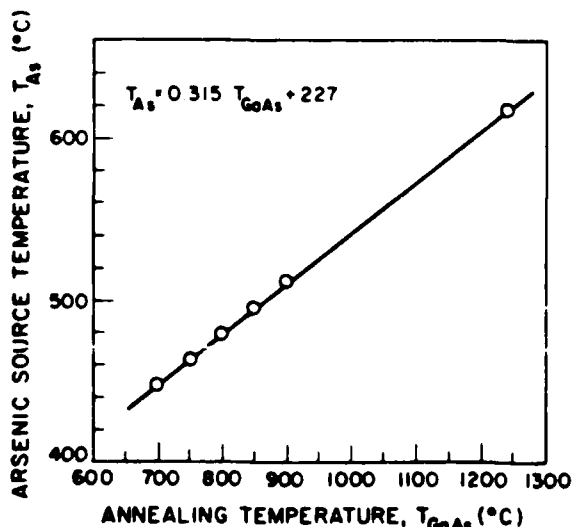


Fig. 5. The linear relationship between annealing temperature ( $T_{GaAs}$ ) and arsenic source temperature ( $T_{As}$ ) for the borderline separating good and bad surface morphologies in Fig. 4.

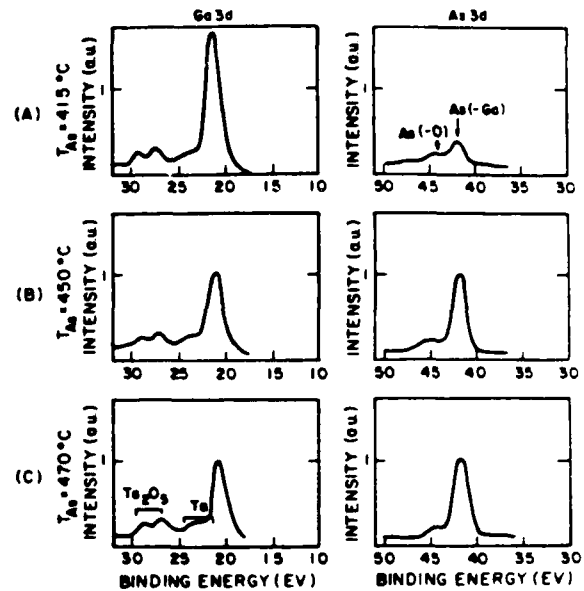


Fig. 6. XPS spectra of Ga 3d and As 3d peaks for the GaAs annealed at 700°C for 16h with arsenic source temperatures of (A) 415°C, (B) 450°C, and (C) 470°C.

(spectra A) exhibit a low intensity As 3d peak and a pronounced Ga 3d peak. This behavior is consistent with preferential arsenic evaporation and the resulting enrichment of the surface with gallium. Spectra B and C correspond to annealing with  $T_{As} = T_{As}^*$  and  $T_{As} > T_{As}^*$ , respectively. It is seen that indeed under these conditions the surfaces remain stable with the As to Ga concentration ratio equal to approximately one. The XPS spectra were taken on "as-annealed" surfaces. It is thus not surprising that they show an additional peak corresponding to arsenic oxide formed probably as a result of exposure to air after annealing. As-related peaks in the vicinity of the Ga 3d peak originate from the specimen holder in the XPS apparatus.

SEM measurements showed that surfaces of GaAs annealed under low arsenic pressure ( $T_{As} < T_{As}^*$ ) contained microscopic inhomogeneities in the form of droplets about 1  $\mu$ m in diam (see Fig. 7). Energy dispersive x-ray spectra shown in the lower portion of Fig. 7 show that the inhomogeneous regions (droplets) correspond to enhanced Ga to As concentration ratio. The linear microscan of an x-ray intensity profile of the Ga K $\alpha$  and As L $\alpha$  lines, respectively, presented in Fig. 8 also shows spatial variations (opposite in phase) of Ga and As concentrations on surfaces annealed with  $T_{As} < T_{As}^*$ . No such variations were detected on surfaces annealed with  $T_{As} > T_{As}^*$ .

Our findings on the compositional and morphological changes of GaAs annealed under different arsenic pressures closely resemble the surface behavior in molecular beam epitaxial (MBE) growth of GaAs (17). Two surface stability regions are considered in MBE, namely, As-stabilized surfaces for high As/Ga flux ratio and relatively low temperatures, and Ga-stabilized surfaces low As/Ga flux ratio and relatively higher temperatures. These results can complement ours, provided two main differences are taken into consideration. One is that the annealing temperature in our study is higher than the typical growth temperature in MBE (usually about 600°C). The other is that only the arsenic flux (controlled by  $T_{As}$ ) is employed in our experiments.

The presently determined equilibrium arsenic pressure data might be useful in actual GaAs device processing. By annealing GaAs under arsenic pressures above equilibrium, the as-annealed GaAs wafers of undegraded surface could be directly transferred to the next steps in the processing without any further surface treatments. However, before visible surface damage occurs, the electrical characteristics might change during heat-treat-

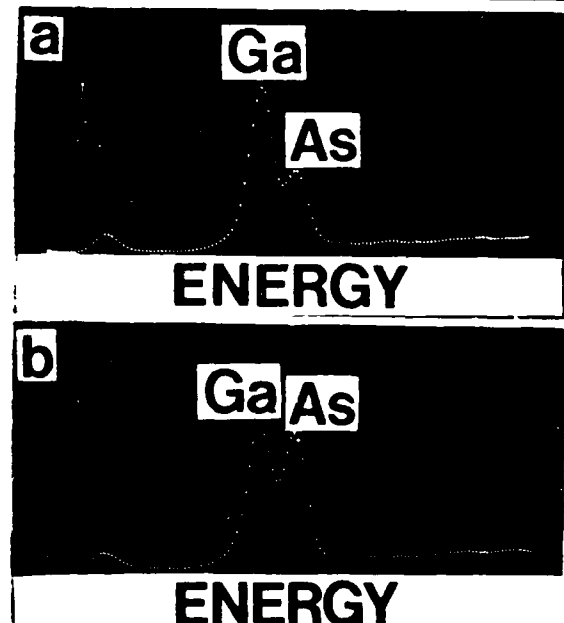
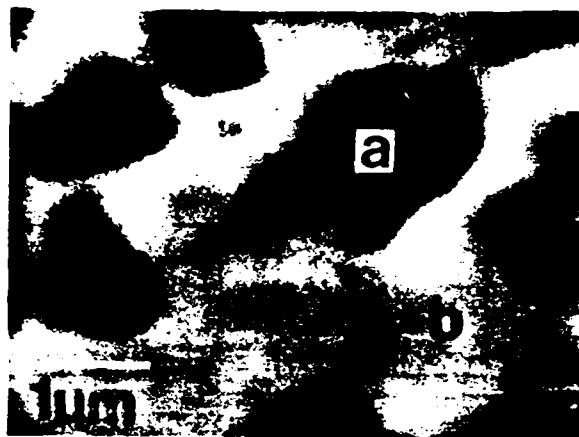


Fig. 7. Scanning electron micrograph of the GaAs surface annealed at 750°C for 16h with  $T_{As} = 440^\circ\text{C}$  and energy dispersive x-ray spectra obtained at the dark droplet (a) and the bright matrix (b).

ments. An extensive study involving the electrical properties of GaAs is currently underway in order to assess the interactions among native defects, impurities, and dislocations during annealing under arsenic ambients.

#### Conclusions

It was determined that during high temperature capless annealing, the surface morphology of GaAs undergoes no detectable changes under ambient arsenic pressure higher than a critical value. This annealing temperature-dependent minimum arsenic source pressure (and thus the minimum arsenic pressure) corresponds to the gas phase equilibrium with a stoichiometric GaAs surface at the annealing temperature. The

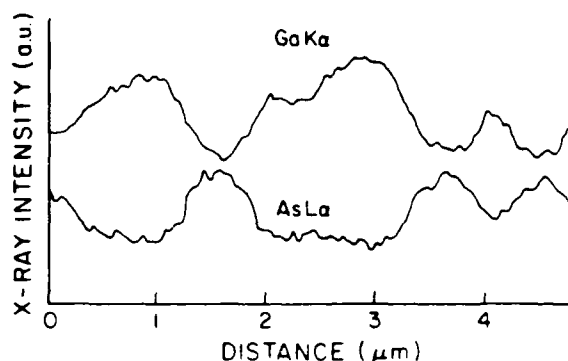


Fig. 8. X-ray intensity profiles of Ga K $\alpha$  and As L $\alpha$  in the middle section of the micrograph in Fig. 7.

critical arsenic source temperatures were determined for various annealing temperatures, and they may be useful in actual GaAs device processing.

#### Acknowledgments

The authors are grateful to the United States Air Force Office of Scientific Research and the National Aeronautics and Space Administration for financial support.

Manuscript submitted April 14, 1986; revised manuscript received Dec. 22, 1986.

Massachusetts Institute of Technology assisted in meeting the publication costs of this article.

#### REFERENCES

1. C. T. Foxon, J. A. Harvey, and B. A. Joyce, *J. Phys. Chem. Solids*, **34**, 1693 (1973).
2. C. W. Farley and B. G. Streetman, *J. Electron Mater.*, **13**, 401 (1984).
3. A. A. Immorlica and F. H. Eisen, *Appl. Phys. Lett.*, **29**, 94 (1976).
4. R. C. Clarke and G. W. Eldridge, *IEEE Trans. Electron Devices*, **ED-31**, 1077 (1984).
5. R. M. Malbon, D. H. Lee, and J. M. Whelan, *This Journal*, **123**, 1413 (1976).
6. C. L. Anderson, K. V. Vaidyanathan, H. L. Dunlap, and G. S. Kamath, *ibid.*, **127**, 925 (1980).
7. F. C. Prince and C. A. Armiento, *IEEE Electron Device Lett.*, **EDL-7**, 23 (1986).
8. J. M. Woodall, H. Rupprecht, R. J. Chicotka, and G. Wicks, *Appl. Phys. Lett.*, **38**, 639 (1981).
9. K. P. Pande, O. A. Aina, A. A. Lakhani, V. K. R. Nair, and J. M. O'Connor, *IEEE Trans. Electron Devices*, **ED-31**, 506 (1984).
10. R. Bhat, B. J. Baliga, and S. K. Ghandhi, *This Journal*, **122**, 1378 (1975).
11. J. Kasahara, M. Arai, and N. Watanabe, *J. Appl. Phys.*, **50**, 541 (1979), and *This Journal*, **126**, 1997 (1979).
12. T. Egawa, Y. Sano, H. Nakamura, T. Ishida, and K. Kaminishi, *Jpn. J. Appl. Phys.*, **24**, L35 (1985).
13. R. P. Mandal and W. R. Scoble, *Inst. Phys. Conf. Ser.*, **45**, 462 (1979).
14. S. J. Pearton, K. D. Cummings, and G. P. Vella-Coleiro, *This Journal*, **132**, 2743 (1985).
15. J. M. Parsey, Y. Nanishi, J. Lagowski, and H. C. Gatos, *ibid.*, **129**, 388 (1982).
16. A. N. Nesmeyanov, "Vapor Pressure of the Elements," p. 451. Academic Press, Inc., New York (1963).
17. A. Y. Cho, *J. Appl. Phys.*, **41**, 2780 (1970), and *ibid.*, **42**, 2074 (1971).



## Optical characterization of semi-insulating GaAs: Determination of the Fermi energy, the concentration of the midgap EL2 level and its occupancy

J. Lagowski, M Bugajski,<sup>a)</sup> M. Matsui,<sup>b)</sup> and H. C. Gatos  
*Massachusetts Institute of Technology, Cambridge, Massachusetts 02139*

(Received 6 April 1987; accepted for publication 17 June 1987)

The key electronic characteristics of semi-insulating GaAs, i.e., the Fermi energy, concentration, and occupancy of the midgap donor EL2, and the net concentration of ionized acceptors can all be determined from high-resolution measurements of the EL2 intracenter absorption. The procedure is based on the measurement of zero-phonon line intensity before and after the complete transfer of EL2 to its metastable state followed by thermal recovery. The procedure is quantitative, involves no fitting parameters, and unlike existing methods, is applicable even when a significant part of the EL2 is ionized.

Electronic parameters of semi-insulating (SI) GaAs and its behavior during device processing depend on the concentration of the native deep donor EL2 and the net concentration of ionized acceptors.<sup>1</sup> Currently, the evaluation of such pertinent parameters is carried out employing a combination of optical and electrical measurements.<sup>1-4</sup> The concentration of EL2 is evaluated from the near-infrared optical absorption, while Hall effect and electrical conductivity measurements yield the Fermi energy from which the EL2 occupancy can be calculated. The concentration of ionized EL2 provides, of course, a measure of the net ionized acceptor concentration. The knowledge of the Fermi energy is crucial, since optical absorption measurements alone cannot differentiate between changes in EL2 occupancy and EL2 concentration. Thus, the reliability of the optical absorption procedure for the determination of the EL2 concentration, as commonly employed, is decreased as the fraction of the ionized EL2 becomes significant, i.e., in *n*-type SI GaAs with resistivities exceeding  $10^6 \Omega \text{ cm}$  and in *p*-type SI GaAs.

In this letter we discuss a characterization approach which is based on measurements of optical absorption, but it is applicable to both *n*- and *p*-type SI GaAs.

The difference between the present approach and earlier approaches is twofold. Firstly, we utilize the EL2 intracenter absorption rather than the total EL2 absorption band. The intracenter absorption is uniquely related to the neutral (occupied) state of EL2 in contrast to the total absorption, in which the photoionization transitions from the occupied EL2 state to the conduction band are involved as well as those from the valence band to the ionized EL2 state.<sup>4,5</sup> Secondly, we utilize the optical excitation of EL2 to its metastable state<sup>6</sup> in order to transfer the entire concentration of EL2 into the neutral state. In the standard approaches the metastable state is used to determine the background absorption which is not related to EL2.<sup>3</sup>

The proposed procedure involves three steps: (1) the SI GaAs sample is cooled in the dark from room temperature to 6 K; (2) EL2 is optically bleached (with white light); and

(3) the sample is annealed at 120–140 K and cooled back to 6 K. The optical absorption spectrum is measured after each step and the corresponding intensities of the zero-phonon line ( $\alpha_{ZPL}^1$ ,  $\alpha_{ZPL}^2$ , and  $\alpha_{ZPL}^3$ , respectively) are used for the quantitative analysis. It is essential that the energy range from 1.037 and 1.041 eV, corresponding to the zero-phonon line,<sup>4,5</sup> is recorded with enhanced resolution and sensitivity.

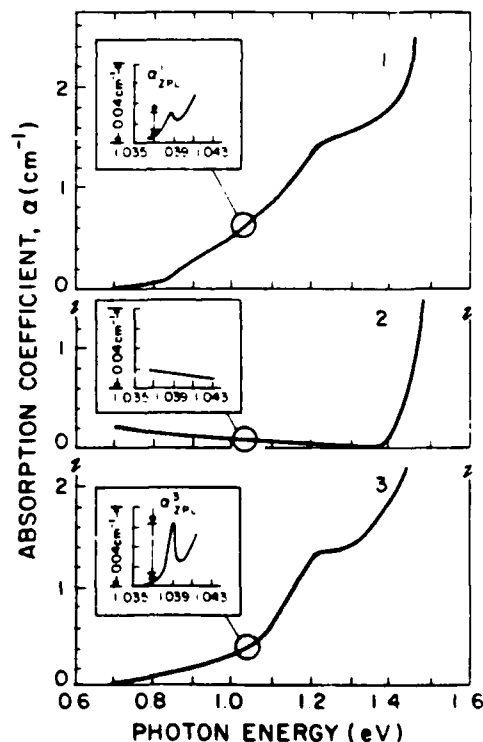


FIG. 1. 6 K optical absorption spectra of GaAs with the EL2 occupancy fraction  $f_0 = 0.3$  at 300 K: 1—after cooling from 300 K, 2—after absorption bleaching, and 3—after subsequent annealing at 140 K for 5 min. Inserts show the zero-phonon line absorption.

<sup>a)</sup> On leave from Institute of Electron Technology, Warsaw, Poland.

<sup>b)</sup> On leave from Sumitomo Metal Mining Co., Ltd., Tokyo, Japan.

Furthermore, the measurements must be carried out with very low intensity incident light in order to prevent any measurable transfer of EL2 into its metastable state during the measurements following steps (1) and (2).

In order to demonstrate the new procedure we take an example of undoped SI GaAs with a relatively low value of Hall effect mobility at 300 K (about  $3000 \text{ cm}^2/\text{V s}$ ) and very high resistivity (about  $5 \times 10^8 \Omega \text{ cm}$ ). In such material a significant fraction of EL2 is expected to be ionized<sup>2</sup> and thus the standard optical method based on Ref. 3 is not readily applicable. The optical spectra taken after steps (1), (2), and (3), and denoted as (1), (2), and (3), respectively, are shown in Fig. 1. Spectrum (1) reflects the ionized state of EL2 frozen from room temperature. This spectrum is different from the EL2 absorption band characteristic of *n*-type conducting GaAs where EL2 is completely neutral. On the other hand, the zero-phonon line (see insert) is clearly observed and provides a measure of the concentration of neutral EL2. Illumination with strong white light [step (2)] eliminates the entire spectrum, including the zero-phonon line (see spectrum 2). EL2 is entirely in its metastable state which is neutral, and optically inactive. Annealing at 140 K for 5 min transforms EL2 back to its normal, optically active, state, without changing its occupancy. As a result, spectrum (3) corresponds to EL2, which is entirely neutral. As can be seen, about a threefold increase in the zero-phonon line intensity is observed in comparison to spectrum (1). The whole absorption band also changes its shape becoming similar to the characteristic absorption of conducting *n*-type GaAs.

The zero-phonon line intensity ratio  $\alpha_{ZPL}^1/\alpha_{ZPL}^3 = f_n$  provides a direct measure of the EL2 occupancy factor  $f_n = n_{\text{EL2}}^0/N_{\text{EL2}}$  (where  $n_{\text{EL2}}^0$  and  $N_{\text{EL2}}$  represent neutral and total EL2 concentration, respectively). The Fermi energy with respect to the bottom of the conduction band becomes  $E_C - E_f = kT \ln(f_n^{-1} - 1) + E_{\text{EL2}}^0$ , where  $E_{\text{EL2}}^0$

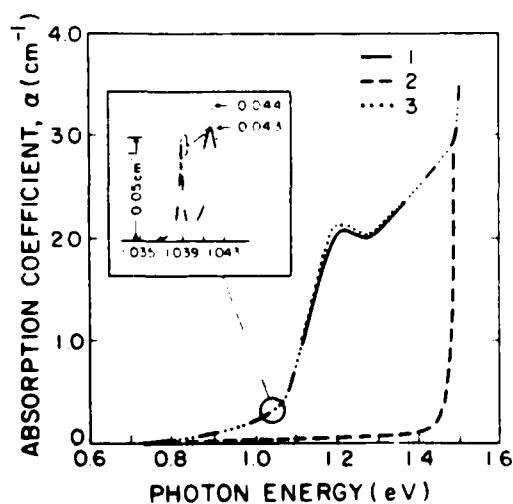


FIG. 2. 6 K optical absorption spectra of standard SI GaAs with majority of EL2 occupied at 300 K. 1, 2, and 3 correspond to the same conditions as in Fig. 1.

$= 0.759 - 0.237 \times 10^{-3} T^{7/8}$  is "effective" EL2 energy which includes a contribution from the degeneracy factor. It must be emphasized that the occupancy factor  $f_n$  or the Fermi energy  $E_f$  can be used to determine the conductivity type and the free electron and hole concentrations.<sup>2,4</sup> If prior to cooling [step (1)], the sample is equilibrated in the dark at 300 K, the  $f_n$  and  $E_f$  values can be taken as representative of this temperature. From existing calculations in Refs. 2 and 9,  $f_n$  and  $E_f$  at 300 K can be related to values of resistivity (or conductivity), free-carrier concentration, and Hall effect mobility.

A recent high-resolution optical and transient capacitance study<sup>4</sup> of EL2 provided a quantitative relation between  $\alpha_{ZPL}$  and  $n_{\text{EL2}}^0$ , i.e.,  $\alpha_{ZPL}/n_{\text{EL2}}^0 = 1.1 \times 10^{18} \text{ cm}^{-1}$ . This ratio is insensitive to temperature between 2 to 10 K. The total EL2 concentration estimated from  $\alpha_{ZPL}^1$  becomes  $N_{\text{EL2}} = 0.9 \times 10^{18} \alpha_{ZPL}^1$ . The concentration of ionized EL2 is given by  $n_{\text{EL2}}^+ = 0.9 \times 10^{18} (\alpha_{ZPL}^3 - \alpha_{ZPL}^1)$ . Considering electrical neutrality, the net concentration of ionized acceptors we have is  $N_A - N_D^+ = n_{\text{EL2}}^+$  (where  $N_D^+$  refers to ionized donors other than EL2).

For example, the set of electrical parameters evaluated from optical measurements for the crystal analyzed in Fig. 1 is as follows:  $N_{\text{EL2}} = 1.5 \times 10^{16} \text{ cm}^{-3}$ ,  $n_{\text{EL2}}^0 = 5 \times 10^{15} \text{ cm}^{-3}$ ,  $N_A - N_D^+ = 1.0 \times 10^{16} \text{ cm}^{-3}$ ,  $f_n = 0.3$ ,  $E_C - E_f = 0.73 \text{ eV}$ ,  $\rho(300 \text{ K}) = 7 \times 10^8 \Omega \text{ cm}$ ,  $\mu_H \sim 3500 \text{ cm}^2/\text{V s}$ ,  $\rho(300 \text{ K}) = 5 \times 10^8 \text{ cm}^{-1}$ . We should point out that conductivity and Hall effect measurements yielded resistivity and Hall effect mobility values within 20% from above estimates.

Application of the present approach to different SI GaAs with high Hall effect mobility ( $\mu_H > 5000 \text{ cm}^2/\text{V s}$ ) and relatively low resistivity (300 K resistivity below  $10^7 \Omega \text{ cm}$ ) is illustrated in Fig. 2. In such material the majority of EL2 is expected to be neutral. Indeed, only a very small enhancement of the zero-phonon line intensity was observed after step (3). Actually, the ratio  $f_n = \alpha_{ZPL}^1/\alpha_{ZPL}^3 = 0.98$  implies that only 2% of EL2 is ionized. Quantitative analysis yields the following values of the other parameters:  $E_C - E_f = 0.64 \text{ eV}$ ,  $N_{\text{EL2}} = 3.6 \times 10^{16} \text{ cm}^{-3}$ ,  $n_{\text{EL2}}^0 = N_A - N_D^+ = 1.6 \times 10^{15} \text{ cm}^{-3}$ . In this case the standard

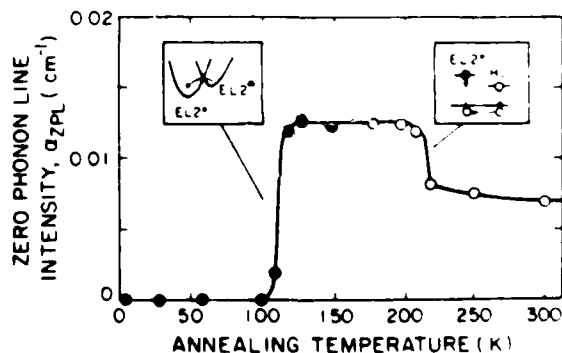


FIG. 3. Zero-phonon line intensity vs the annealing temperature of step (3) used to recover the EL2 from the metastable state. Filled and open circles correspond to annealing time of 10 and 15 min, respectively.

method for the determination of EL2 concentration from the total optical absorption at  $\lambda = 1.06 \mu\text{m}$  can be conveniently employed. Indeed, this standard method yielded  $N_{\text{EL2}} = 3.4 \cdot 10^{16} \text{cm}^{-3}$  (using the revised calibration factor after Ref. 4) in very good agreement with the present approach.

It should be pointed out that EL2 is the dominant midgap level in GaAs crystals grown by the standard methods from As-rich melts.<sup>7</sup> Other midgap levels are present, but at concentrations about one magnitude smaller than that of EL2. Since the zero-phonon line employed here is uniquely related to EL2 with a specific signature,<sup>8</sup> our approach for the determination of the EL2 concentration remains valid, even in the presence of other midgap levels at concentrations comparable to those of EL2. In such a case, however, the concentration of ionized EL2 cannot be taken as an exact measure of concentration of the net ionized acceptors but rather as the lower limit of  $N_A - N_D^-$ .

In the course of this investigation we found that the intensity of the zero-phonon line,  $\alpha_{\text{ZPL}}^1$ , reaches a constant value for annealing temperatures  $T_A > 120 \text{ K}$ , consistent with the established EL2 behavior in SI GaAs. Beyond 220 K, however,  $\alpha_{\text{ZPL}}^1$  decreases significantly, as shown in Fig. 3. Measurements of thermally stimulated current (TSC) showed that this decrease is associated with the thermal emission of holes (trapped during illumination at low temperatures by hole traps HL3, HL9, and HL10)<sup>10</sup> and their recombination with EL2 electrons. Thus, if relatively shallow hole traps are present at high densities, a decrease of  $\alpha_{\text{ZPL}}^1$  can in general take place. This potentially interfering process can be recognized (using additional TSC measurements) and minimized by adjusting the annealing conditions, i.e., temperature and annealing time.

In summary, we have shown that high-resolution measurements of the 1.039 eV zero-phonon line can be very effectively applied for the optical characterization of SI GaAs. This approach has fundamental advantages over the standard optical method for the determination of the EL2 concentration in the characterization of materials in which EL2 is partially ionized. It should prove particularly useful in the characterization of a new type of GaAs crystal exhibiting inverted thermal conversion (ITC) in which very high resistivity is achieved by thermal annealing.<sup>11</sup> The standard optical method is not suitable for ITC GaAs because in this material a significant fraction of EL2 is ionized.

The authors are grateful to the National Aeronautics and Space Administration and to the Air Force Office of Scientific Research for financial support.

<sup>1</sup>G. M. Martin, J. P. Farges, G. Jacob, and J. P. Hallais, *J. Appl. Phys.* **51**, 2840 (1980).

<sup>2</sup>W. Walukiewicz, J. Lagowski, and H. C. Gatos, *Appl. Phys. Lett.* **43**, 192 (1983).

<sup>3</sup>G. M. Martin, *Appl. Phys. Lett.* **39**, 747 (1981).

<sup>4</sup>M. Skowronski, J. Lagowski, and H. C. Gatos, *J. Appl. Phys.* **59**, 2451 (1986).

<sup>5</sup>M. Kaminska, M. Skowronski, and W. Kuszko, *Phys. Rev. Lett.* **55**, 2204 (1985).

<sup>6</sup>G. Vincent, D. Bois, and A. Chantre, *J. Appl. Phys.* **53**, 36 (1982); H. C. Gatos and J. Lagowski, *Mater. Res. Soc. Symp. Proc.* **46**, 153 (1985).

<sup>7</sup>The revised value of the EL2 electron emission activation energy is used after Ref. 7. This value is slightly lower (by 10 meV) than the value used in Ref. 1.

<sup>8</sup>J. S. Blakemore, *J. Appl. Phys.* **53**, R123 (1982).

<sup>9</sup>G. M. Martin, in *Semi-Insulating III-V Materials*, edited by G. J. Rees (Shiva, Orpington, U.K., 1980), p. 13.

<sup>10</sup>J. Lagowski, H. C. Gatos, C. H. Kang, M. Skowronski, K. Y. Ko, and D. G. Lin, *Appl. Phys. Lett.* **49**, 892 (1986).

DATE  
FILMED  
8